IMPROVING THE BIOCOMPATIBILITY OF STAINLESS STEEL SURFACES THROUGH SILANE POLYETHYLENE GLYCOL COATINGS

M.Sc. Thesis
Ville Hynninen
BioMediTech
University of Tampere
September 2014

PRO GRADU -TUTKIELMA
Paikka: TAMPEREEN YLIOPISTO
BioMediTech
Tekijä: HYNNINEN, VILLE JOHANNES
Otsikko: Ruostumattomien teräspintojen bioyhteensopivuuden parantaminen silaanipolyetyleeniglykoli-pinnoitteilla
Sivumäärä: 60 sivua, 5 hakemistosivua
Ohjaajat: Dosentti Vesa Hytönen ja Jenita Pärssinen, FT
Tarkastajat: Prof. Markku Kulomaa ja Dosentti Vesa Hytönen
Aika: Syyskuu 2014

Tiivistelmä

Biologisissa ympäristöissä orgaanisen materiaalin epäspesifistä kertymistä pintarakenteisiin on usein mahdotonta välttää. Tyypillisesti sitä pidetään haitallisena, koska se lisää esimerkiksi patologisten kontaminaatioiden riskiä lääketieteellisissä ympäristöissä sekä koneiden ja teollisuuden laitteiden huolto- ja korjaustarvetta. Siksi pinnat, jotka pystyisivät säätelemään biologisten aineiden kertymistä, olisivat erittäin hyödyllisiä lukuisissa käytännön sovelluksissa. Lisäksi pintarakenteet, jotka samanaikaisesti mahdollistaisivat tiettyjen molekyylien tai partikkeleiden hallitun sitoutumisen, edelleen laajentaisivat kyseisten pintamateriaalien käyttömahdollisuuksia esimerkiksi biosensorien ja bioteknologisten laitteiden kehityksessä.

Tässä Pro Gradu -tutkielmassa ruostumattomia teräspintoja pinnoitettiin silaanipolyetyleeniglykolijohdannaisilla (silaani-PEG), jotta voitaisiin arvioida silaani-PEG:ien soveltuvuutta teräspintojen muokkaukseen sekä tuotetun pinnoitteen laadun että myös saavutetun toiminnallisuuden kannalta. Ruostumaton teräs valittiin käytettäväksi materiaaliksi sen erinomaisten fysikaalisten ominaisuuksien sekä laajan käytettävyyden ja taloudellisen merkittävyyden vuoksi. Silaani-PEG:in puolestaan päädyttiin, koska PEG-ketjujen tiedetään pystyvän vähentämään epäspesifistä sitoutumista ja koska silaaniryhmien avulla pinnoite voitaisiin liittää teräspintaan kovalenttisilla sidoksilla. Muokattujen pintojen laatua ja ominaisuuksia tarkasteltiin pintaherkillä menetelmillä, röntgensädefotoelektronispektroskopialla (XPS) sekä kontaktikulmamittauksilla, ja silaani-PEG:ien havaittiinkin muodostavan ohuen ja melko yhtenäisen pinnoitteen. Lisäksi atomivoimamikroskopiaa (AFM) ja pyyhkäisyelektronimikroskopiaa (SEM) hyödynnettiin tulosten visuaalisessa arvioinnissa.

Valitettavasti pinnoitteen kovalenttista sitoutumista teräkseen silaaniryhmien kautta ei onnistuttu varmistamaan. Siitä huolimatta silaani-PEG:t tarttuivat pintoihin ja vähensivät merkittävästi sekä *E. coli* -bakteerien että kahden erilaisen proteiinin, avidiinin ja fibronektiinin, epäspesifistä kertymistä pinnoille. Täydellistä tarttumisen estymistä ei kuitenkaan havaittu yhdessäkään koejärjestelyistä. Lisäksi silane-PEG -muokattujen pintojen valikoiva jatkomuokkaus osoitettiin mahdolliseksi liittämällä avidiineja silaani-PEG-biotiini -pinnoitteisiin. Näistä kokeista saadut havainnot sekä tarkastellut menetelmät tarjoavat hyödyllisiä työkaluja jatkotutkimuksiin sekä muodostavat tukevan perustan pinnoitetekniikoiden jatko-optimoinnille sekä sovellettavuudelle.

Avainsanat: ruostumaton teräs, silanointi, polyetyleeniglykoli, antifouling-pinnoite, pintamuokkaus, biofunktionalisointi, bioyhteensopivuus, *E. coli*, avidiini

MASTER'S THESIS
Place: UNIVERSITY OF TAMPERE
BioMediTech
Author: HYNNINEN, VILLE JOHANNES
Title: Improving the biocompatibility of stainless steel surfaces through silane polyethylene glycol coatings
Pages: 60 pages, 5 index pages
Supervisors: Docent Vesa Hytönen and Dr. Jenita Pärssinen
Reviewers: Prof. Markku Kulomaa and Docent Vesa Hytönen
Date: September 2014

Abstract

In biological environments nonspecific accumulation of organic material to surfaces is often inevitable. Generally, it is also considered harmful as it, for instance, increases the risk of pathological contaminations in medical settings as well as the maintenance costs of industrial apparatuses. Thus, surfaces that are capable of preventing accumulation of biological substances, i.e. biofouling, would be of huge benefit for various practical applications. In addition, surfaces, that would simultaneously allow selective binding of certain types of molecules or particles, would furthermore broaden the scope of possibilities, for example, in developing biosensors and biotechnological equipment.

In this thesis stainless steel surfaces were coated with layers consisting of silane polyethylene glycol (silane-PEG) derivatives in order to examine the suitability of the silane-PEGs for stainless steel modification in terms of both the quality of the obtained surface coatings and achieved functionality. Stainless steel was selected because of its remarkable physical properties and its role as one of the most significant and diversely used metallic substance. Silane-PEGs were chosen because PEG chains are known to be able to prevent nonspecific adsorption and, additionally, the silane groups would provide an excellent way of coupling them covalently to the surfaces. The quality and characteristics of the modified surfaces were investigated with surface sensitive methods, X-ray photoelectron spectroscopy (XPS) and contact angle measurements, and the silane-PEGs were found to form a thin and rather uniform layer on the surfaces. Also atomic force microscopy (AFM) and scanning electron microscopy (SEM) were used for visual assessment.

Unfortunately, though, the covalent bonding of the coating via the silane groups could not be confirmed. Nevertheless, the silane-PEGs attached firmly to the surfaces and were able to significantly reduce the nonspecific accumulation of both *E. coli* bacteria and two different kinds of protein, avidin and fibronectin. In any of the cases, though, complete prevention of attachment was not achieved. Additionally, the further selective functionalization of the silane-PEGs was shown to be possible by linking avidins to silane-PEG-biotin modified steel surfaces. The observations made from these experiments and the tested methods themselves provide a useful set of tools for future studies and form a solid foundation for further optimization and applicability of the coating techniques.

Key words: stainless steel, silanization, polyethylene glycol, antifouling coating, surface modification, biofunctionalization, biocompatibility, *E. coli*, avidin

Acknowledgements

Firstly, I would like to show my gratitude to Vesa Hytönen and Mika Valden who were willing to put their faith in me and allowed me to challenge myself and to take on this project. Without them this thesis would never have seen daylight. Vesa, as one of my instructors, has also been a never-ending source of optimism and provided me with excellent ideas and advice as well as valuable feedback.

Another huge thanks goes to my other instructor Jenita Pärssinen, whose open-mindedness and guidance was priceless in solving various practical issues and in designing and fine-tuning many of the experiments. Her positive attitude and encouragement for ”out of the box” thinking especially kept the project interesting and my motivation going despite some less inspiring and monotonous lab days.

One important thank you goes also to the personnel of the Protein Dynamics Group and the Surface Science Lab, with whom I was privileged to work for the duration of this thesis. I could not have hoped for a better place to work on this project. In particular, I would like to thank Markku Hannula, Leena Vuori and Elina Lehtonen, whose skills and knowhow were priceless in sample preparing and especially in the XPS measurements. In addition, Markku and Elina deserve a special thanks for performing the actual analysis of the XPS data. An additional thanks goes also to a fellow-student Taina Viheriälä for precious peer support and cheering conversations during long days of lab work and writing.

Lastly, I’d like to thank all of the collaborators, who have lent me their expertise and equipment and, thus, significantly helped me and simultaneously contributed to this thesis. A big thanks goes to Kosti Tapio and Tommi Isoniemi from the Molecular Electronics and Plasmonics group (University of Jyväskylä) led by Jussi Toppari, who took care of the AFM and SEM imaging of the samples and then also provided expert commentary and feedback about the results. Likewise, I’m also in gratitude to Merja Ritola and the Department of Material Science (Technical University of Tampere), who allowed me to use their contact angle measurement equipment.

Contents

1 Introduction

Compatibility and interactivity of surfaces with their surroundings are critical for a wide range of applications. Especially, from the point of view of medical technology and biotechnological applications the ability to specifically control and modify the biocompatibility of surfaces would be highly beneficial (Michu et al. 2011; Parbhu et al. 2006; Petrone 2013). Additionally, in food and marine industry, for example, the reduction or prevention of undesired biofouling and microbially influenced corrosion are goals pursued with tailor-made and functionalized surfaces (Videla and Characklis, 1992; Maller 2007). However, new materials with both desired surface properties and appropriate bulk properties are usually not readily discovered or available and it is, therefore, often preferable to modify the surfaces of existing otherwise potential materials, e.g. stainless steel (Maller 2007). Thus, through chemical or physical modifications it is possible to adjust a particular material to comply with diverse circumstances. For instance, covalent cross-linking and grafting of polymers provide a myriad of options to customize the biocompatibility and capabilities of otherwise biologically compromised materials (Benhabbour et al. 2008; Tabary et al. 2007).

In particular, biomedical materials used, for example, in orthopedic implants are extremely tempting targets for modifications, since their surfaces are constantly exposed to body fluids and compounds, and the well-being of the patient relies on the proper interplay between the implant and the host body. Hence among others, improved resistance to biofouling and consequently to possible biomaterial-associated infections are attractive goals worth pursuing. (Al-Ahmad et al. 2013; Gallo et al. 2003; Subbiahdoss et al. 2008).

However, the properties and events that determine the significance and the extent of the material's interactions with its environment, e.g. with proteins and cells in biological surroundings, are deeply complex. For instance, nano- and microscale topographies, chemical and physical properties and the mechanics of the surface as well as the cell-material interface contribute to the activity and biomimetics of surfaces and it is indeed their combinatory effect that typically defines the overall surface characteristics (Gonzáles-García et al. 2010; Guégan et al. 2014; Xu et al. 2007; Yang et al. 2014). For the time being, however, the whole picture and all aspects of the cooperativity are still elusive and unclear, which makes the studying of surface reactions

somewhat challenging (Rabe et al. 2011). However, one representative and common experimental method used to adjust and control the biocompatibility of materials is to coat their surfaces with grafted polymer chains. Especially polyethylene glycols (PEG) are broadly utilized and at the moment they are also one of the most widely used choice for controlling cell-biomaterial interactions (Kingshott and Griesser, 1999).

In this thesis stainless steel surfaces were modified with coatings consisting of silane-PEG derivatives in order to study how the fouling properties and the functionality of the surfaces could be adjusted through these modifications. At first, in the review of the literature section the diversity of the factors affecting surface fouling are represented with an emphasis on protein and bacterial adsorption. In biological surroundings the protein accumulation is typically considered as the first stage of fouling, which further enables bacterial and cellular attachment (Wei et al. 2003). Antifouling surfaces are also discussed, with a focus on PEG-grafted surfaces, to elucidate the theoretical background of the practical experiments. Later, the experimental setup and results are represented and then, lastly, discussed and concluded.

2 Review of the literature

2.1 Biofouling

Biofouling can be defined as irreversible and uncontrolled adhesion and accumulation of biological substances on synthetic surfaces. When considering biomedical applications the amount of the adsorption of proteins is often reckoned to be the standard with which the biocompatibility of materials is measured and compared as well as the primary target to be prevented, as biofouling is generally regarded harmful (Kingshott and Griesser, 1999). However, cells typically need adsorbed proteins in order to adhere to foreign materials, and the proteins, when in their native conformations, are able to greatly affect adhesion, migration and proliferation of cells on various surfaces (Benhabbour et al. 2008; Gonzáles-García et al. 2010). On the other hand though, if proteins denature as a consequence of adsorption in an uncontrollable manner and if bacteria are able to attach on surfaces, an implant, for instance, most likely will not be able to replicate the actual biological structure and function at that body site as intended, which may provoke adverse biological responses, e.g. fibrous encapsulation, thrombosis and inflammations (Kingshott and Griesser, 1999). The bacteria may also form biofilms that are capable of resisting native immunodefences as well as pharmaceutical treatments (Michu et al. 2011). Thus, methods to guide and control protein and cell adsorption are eagerly sought after.

2.2 Factors involved in protein adsorption

2.2.1 Environmental factors

The adsorption behavior of proteins is considerably influenced by the surrounding conditions that essentially include temperature, pH and the electrochemical and ionic composition of the buffer (Demanéche et al. 2009; Jones and O'Mella 2000; Rabe et al. 2011). Alterations in temperature affect both the equilibrium state and the overall adsorption kinetics of proteins as well as their stability. In general, higher temperatures are expected to lead to higher protein adsorption rates, since diffusion of the proteins is increased and, thus, contacts between the proteins and the sorbent surface become more frequent. Moreover, alterations in the temperature also influence the stability of the proteins, which may further affect their adsorption behavior (Rabe et al. 2011). Nonetheless, following protein adsorption water molecules and other adsorbed small molecules or particles are released from the surface and replaced by the proteins. As a

result, entropy, that is considered to be the driving force of the protein adsorption, is increased (Koutsoukos et al. 1983; Rabe et al. 2011). Additionally, proteins often undergo structural rearrangements following adsorption which further thermodynamically favors the process (Norde 1996).

2.2.1.1 pH of the environment

The pH is related to the protein adsorption, since it has an effect on the electrostatic state of the proteins. The charge of protein molecules is dependent on the relationship between the pH and the isoelectric point (pI) of the proteins (Demanèche et al. 2009; Rabe et al.2011). At low pH (pH<pI) the proteins are positively charged, whereas high pH (pH>pI) generates negatively charged molecules. When pH equals pI, the charges cancel out each other and the proteins bear no net charge (Demanéche et al. 2009). Typically in terms of the adsorbed mass, the protein adsorption is most efficient at the isoelectric point since the electrostatic repulsions are minimized or possibly completely avoided. On the other hand though, charged proteins are able to attach more tightly to oppositely charged surfaces through electrostatic interactions. These attractive forces are extremely significant as they effectively guide proteins to the surfaces, even though repulsive charges between the proteins do not allow as dense packing as would be possible in the pI conditions (Demanéche et al. 2009). In addition, the electrochemical properties of solvent affect the adsorption and packing of the proteins as, for example, salt ions regulate the strength and range of the repulsive or attractive forces and, thus, ought to be taken into account as well (Jones and O'Melia 2000).

2.2.1.2 Ionic strength

The composition of the solvent, particularly the ionic strength, influences inter- and intramolecular forces of the solutes and, thus, has an impact on e.g. electrostatic protein-protein repulsions, packing density and possible protein aggregation (Demanéche et al. 2009; Jones and O'Melia 2000). In general elevated salt concentration dampens the repulsion between like-charged molecules and, hence, allows higher packing density and more effective adsorption. On the other hand though, as a consequence of increased electrolyte concentration the electrostatic attractions are likewise reduced (Jones and O'Melia 2000). As a practical example, the ”Hofmeister-series”, i.e. a categorization of ions based on their ability to precipitate or solubilize proteins, and the related salting out

effect that are utilized in protein purification, are based on the knowledge on ionic composition and strength of solvents and their effects (Kunz et al. 2004). Interestingly, also non-ionic surfactants, such as Tween20, affect the adsorption and organization of proteins on surfaces rather similarly, with the exception that instead of adjusting the electrical conditions the effect is caused by alterations in hydrophobic interactions (Pellenc et al. 2006).

2.2.2 Surface related factors

The surface properties that significantly affect protein adsorption are surface polarity, electrical charge and morphology (Demanéche et al. 2009; Gonzáles-García et al. 2010; Xu and Siedlecki 2007). These characteristics can and will oftentimes be controlled, for instance, through silanization or polymer grafting, to achieve better and more suitable surface materials e.g. for medical applications (Becker et al. 2006; Tabary et al. 2007). Hence, modifications broaden the scope of applications in which a material can be used.

In general, more hydrophilic and electrically neutral surfaces are considered to be inert and capable of resisting protein adsorption. Also, the amount of hydrogen bond acceptors and donors affect the surface inertness, although the results are not completely unanimous. In most cases though, the surfaces that bear hydrogen-bond acceptors and lack hydrogen-bond donors are more resistant to biofouling (Ostuni et al. 2001). Nevertheless, Luk et al. (2000), for instance, have reported that self-assembling monolayers presenting mannitol groups are also resistant to protein adsorption regardless of the existence of a large number of hydrogen-bond donors. Additionally, when considering glycoproteins whose more hydrophobic protein core is shielded with hydrophilic glycans, a deviation in adsorption behavior can be noticed. Due to their oligosaccharide shells, the glycoproteins preferentially adsorb on hydrophilic surfaces as opposed to other, unmodified proteins (McColl et al. 2007). Thus, the adsorption of proteins is not only dependent on the surface properties, but may be considered as an interplay between the characteristics of the particular protein and the surface.

2.2.2.1 Surface topography

The relationship between the topography of the surface and protein adsorption is not completely clear even though in some cases the roughness of the surface has been shown to have some effect for the adsorption. For instance, González-García et al.

(2010) have demonstrated that the amount of adsorbed fibronectin on poly(L-lactic acid)polystyrene surfaces of different nanotopographies varies with the surface roughness and also that these different surfaces, when expressing uniform densities of fibronectin, affect dissimilarly the focal adhesion formation and the attachment of MC3T3 cells. Thus, the surface nanotopography seems to regulate protein adsorption and the cell adhesion thereafter. These notions were also supported by Lord et al. (2010), who claimed that nanotopographies of surfaces significantly affect protein adsorption. Nonetheless, they also pointed out that different kinds of surfaces may influence the behavior of different proteins dissimilarly and, additionally, that in some occasions, when considering surfaces modified with certain proteins, cells may not necessarily react to the surface-grafted proteins as intended, but may rather be guided by the randomly adsorbing proteins originating from growth medium or serum instead. As a case in point, Cai et al. (2006) have studied albumin and fibronectin adsorption, as well as, osteoblast proliferation and viability on titanium films of varying nanometre scale topographies, and as opposed to the observations made by González-Garcia et al. (2010), they detected no statistically significant differences neither in protein adsorption nor in cell behavior as a function of surface roughness. Thus, the surface roughness can be said to affect the adsorption behavior of proteins to some extent and in certain cases, although at the moment unanimous conclusions cannot be drawn and the final outcome may be dependent on specific case by case factors.

2.2.2.2 Surface hydrophilicity

Xu and Siedlecki (2006) have investigated how surface wettability and protein exposure time affect the adsorption of three blood plasma proteins, bovine serum albumin (BSA), fibrinogen and human FXII, on low density polyethylene (LDPE) surfaces that were plasma treated to obtain different levels of wettability. They showed that for all three proteins notably stronger adhesion forces were observed on hydrophobic LDPE surfaces with measured contact angles of 60° and higher than on more hydrophilic surfaces with contact angle values below 60°. In short, a distinct transition in protein adsorptivity from weakly adherent to adherent was observed when crossing a contact angle limit of approximately 60° to 65°. Moreover, changes in the wettability and contact angle did not seem to have significant effects on the adsorption behavior unless the changes occurred across the above mentioned 60° limit which further highlights a step

dependence in protein adhesion force at the contact angle region of 60°-65°. Hence, minor changes and the adjusting of the wettability may not be particularly useful tool in controlling protein adsorption on surfaces unless a transition across the 60°-65° region is achieved. This hypothesis is also supported, for example, by the studies performed by Yoon et al. (1997) and Berg et al. (1994) who have suggested that hydrophobic attractive forces are poorly supported or not observed at surfaces with contact angles below 62.5° and 65°, respectively. Moreover, since the plasma treatment is known to affect LDPE surface roughness in addition to the wettability characteristics, the rather constant adhesion forces measured among all of the wettable and non-wettable surfaces implied that minor alterations in the surface topography and roughness do not considerably affect protein adsorption (Xu and Siedlecki 2006).

2.2.3. Protein related factors

Proteins consist of 20 different naturally occurring amino acids and additionally may have different kinds of post-translational modifications, such as phosphate groups and oligosaccharide chains, which further contribute to their complex structures and features. Thus, each protein has its own unique molecular personality, which determines how it reacts with the surroundings and ultimately also characterizes the adsorption behavior of the protein. For instance, the electrostatic nature of the molecule and the interfacial activity as well as the interactions between the protein domains contribute to the distinctive characteristics of the proteins (Andrade et al. 1992). Consequently, a unified theory of protein adsorption is still far from being achieved, even though the overall major contributors, at least from the thermodynamical point of view have been somewhat recognized. The primus motors of the adsorption process are acknowledged to include reorganization of charged groups, beneficial dispersion forces between the proteins and the surface, alterations in the hydration state of the proteins and the surface as well as structural rearrangements of the adsorbing proteins (Norde 2008).

2.2.3.1 Hard and soft proteins

In terms of the interfacial behavior the proteins can be classified according to their structural properties, i.e. size, stability and composition, to narrow down the immense diversity. The proteins may be sorted as either hard or soft (Norde 1996; Norde 2008). This is related to the notion that proteins fold to achieve their free energy minimum, and

this energy minimum along with the preferred conformation is often different for a free-floating protein in a solution than for a protein that is in contact with a surface. In other words, the classification is basically based on the size and the internal cohesion of the proteins and roughly describes how probable it is for the proteins to undergo structural rearrangements upon a contact to a surface (Norde 1996). Small and rigid proteins, e.g. lysozyme and β-lactoglobulin, are referred to as hard proteins, since they are not typically structurally remodeled following a surface adsorption, i.e. they are highly stabile (Norde 2008; Rabe et al. 2011). As a consequence, hard proteins do not normally adsorb particularly well on hydrophilic surfaces, unless they are electrostatically attracted (Norde 2008). Soft proteins are structurally more loose and labile than the hard proteins and, hence, tend to reorganize upon surface adsorption. Oftentimes they are also larger and contain multiple subunits and domains (Norde 2008; Rabe et al. 2011) Remodeling of these proteins may also include unravelling of ordered secondary structures. As a result, the increase in entropy may in some occasions be enough to facilitate the adsorption of the soft proteins onto even electrostatically incompatible surfaces (Norde 2008). One may, thus, consider soft proteins being *sticky*.

2.2.3.2 Protein adsorption kinetics is seldom straightforwardly linear

The adsorption behavior of protein mixtures is dependent on the diffusion and adsorption characteristics of the proteins as well as the repulsion processes between the proteins themselves and the proteins and the surface (Rabe et al. 2011). In an early adsorption stage the most prominent operators are the small proteins due to the fact that they diffuse faster than the large ones and, consequently, are more eligible to interact with the surface. Thus, the concentration of the faster and smaller proteins reaches a certain local maximum until other proteins arrive. In later stages some of the smaller proteins are replaced by other less motile and bigger proteins that have higher surface affinity, hence the adsorption kinetics do not oftentimes follow simple linear growth (Hirsh et al. 2013). This competitive replacement of adsorbed proteins is called "Vroman effect" after Leo Vroman in recognition to his initial groundbreaking studies on the subject with blood plasma proteins (Vroman and Adams 1969; Vroman et al. 1971; Vroman et al.1980).

However, transient adsorption maxima, i.e. overshoots in adsorption kinetics, are not only observed in mixtures of proteins but in solutions consisting of only one

type of protein as well (Daly et al. 2003; Ohshima et al. 2004; Wertz and Santore 2002). One general model that is used to explain this kind of behavior is the "time delay model" that is utilized in colloid and polymer adsorption studies (Ohshima et al. 1992; Ohshima et al. 2004). According to the model, desorption of the molecules does not begin simultaneously or immediately following the first adsorption events, but instead requires a certain time delay to take place. The desorption is initiated through the conformational changes in the adsorbed molecule layer and, thus, a temporary overshoot may be reached before desorption begins and allows the adsorption to become equilibrated (Ohshima et al. 2004). Even though the delay model recognizes the overshoot effect, and the proteins, in fact, are massive biopolymers, more protein-specific and extensive explanations are being searched. The above mentioned Vroman effect is one of the concepts created to rationalize protein adsorption behavior.

For instance, Wertz and Santore (2002) and Daly et al. (2003) have witnessed overshoot effects in lysozyme adsorption behavior. Both studies suggest that the initial adsorption of the enzyme occurs in so-called end-on conformation, which is then followed by a transition into a side-on conformation on the surface. The side-on conformation is considered to be energetically more favorable but it also requires more surface space than the end-on conformation. Hence, the transitional adsorption maximum is concluded to be a consequence of a situation when adsorption rate exceeds the transition rate of the end-on - side-on orientational change and, therefore, the end-on oriented proteins start to accumulate. However, even though both groups assessed the adsorption of lysozyme through the same fluorescent label in very similar experimental settings, their conclusions were otherwise divided, apart from the mentioned conformational rearrangement. Wertz and Santore (2002) state that the intensity loss after the overshoot maximum is a result of displacement of the more confined end-on oriented proteins by energetically more stable side-on proteins which leads to releasing of labeled proteins from the surface. However, Daly et al. (2003) propose that the observed drop in intensity is purely an inherent defect in the experimental setup since the orientational rearrangement of the proteins partially quenches the fluorescent signal. Thus, the proteins are not necessarily released from the surface after all. However, none of the groups has actually investigated the claimed differences in the surface affinities of the end-on and side-on conformations and, thus, lack some important supportive data for their conclusions as Rabe et al. (2011) pointed out.

In addition, one theoretical explanation for the peculiar adsorption phenomena is also suggested by Rabe et al. (2007) for which they also show experimentally acquired confirmative data. The model combines the above mentioned delay model as well as the idea of essential orientational or conformational rearrangements: In short, the adsorbed proteins are initially in a conformation that disfavors desorption and only after an adsorption of certain amount of proteins they are transformed into another form which facilitates the desorption. Thus, a delay is observed before the start of desorption, since proteins cannot desorb until enough desorption-enabling and -stimulating protein-protein and protein-surface interactions are formed.

2.3 Introduction to materials and methods used in this study

2.3.1 Stainless steel

Stainless steel (SS) is widely used and accepted as biomaterial because of its great mechanical properties, durability, corrosion resistance and good workability as well as low corrosiveness and costs compared to other metals (Maller 2007; Ren et al. 2005). Additionally, a natural oxide layer forms on stainless steel surfaces, which contributes to the characteristic "stainless" quality, and it is also adequately biocompatible already by itself (Ren et al. 2005; Talha et al. 2013). In fact, austenitic stainless steels, such as AISI 316, which was also used in this study, are the most widely utilized materials for orthopedic applications (Talha et al. 2013).

2.3.2 Polyethylene glycol

Polyethylene glycol (PEG) is a linear or branched neutral polyether that exists in a multitude of molecular weights, i.e. chain lengths. It is sometimes also referred to as polyethylene oxide (PEO), poly(oxyethylene) (POE) or poluoxirane, depending on the size of the molecule or how the constituent monomer is determined. In biological terms, PEG possesses many remarkable properties. Most importantly, PEG is able to efficiently exclude other polymers from adjoining surroundings in an aqueous environment. However, PEG is also soluble in many organic solvents, for example toluene and methylene chloride. In addition, PEG layers repel proteins from their presence, the layers are immiscible to other polymers and form two-phase systems with them and are also nonimmunogenic and nonantigenic. Moreover, PEG polymer can be readily attached to other molecules and it is able to react with surfaces and cell

membranes. Nonetheless, PEG is nontoxic and does not harm active proteins or notably affect the chemistry of other molecules linked to it, even though their solubility and molecular size are altered as a result of the coupling (Harris 1992). As a drawback, though, PEG can be auto-oxidized in the presence of transition metal ions, which are included in most biochemically relevant solutions, and oxygen. Also in *in vivo* conditions alcohol dehydrogenase enzymes are able to oxidize the terminal hydroxyl group of PEGs to aldehyde groups, which can either be further oxidized or possibly react with proteins, for instance (Kane et al. 2003; Ostuni et al. 2001).

2.4 Grafted polymers adjust the biomimetics of surfaces

In addition to pure antifouling surfaces, also surfaces with specific binding and activity patterns are sought after. Moreover, it would oftentimes be beneficial to combine the two properties, antifouling on one hand and selective binding tendency on the other, in one material (Kasemo 2002). One of the most successful and most extensively used method to achieve this dualistic behavior is to graft polymer molecules on the surfaces and possibly further couple other specific molecules onto the polymers. Especially PEG has proved to be a very potential and triumphant grafting material in terms of both of the desired properties; the reducing of non-specific binding and enabling the selective functionalization as well. Therefore, PEG is one of the most broadly used polymer for controlling biomaterials' interactions with the surroundings (He et al. 2014; Kingshott and Griesser 1999; Sonato et al. 2013). Thanks to multiple different grafting methods PEGs can also be attached to a variety of materials with distinctive properties, and in this thesis, for example, PEGs were attached to stainless steel surfaces via silane mediated covalent bonding.

2.4.1 How PEGylated surfaces resist protein adsorption?

Even though the actual mechanism of the biofouling resistance of PEG coated surfaces has not been completely solved, promising models and hypotheses have been developed. For example, Andrade and de Gennes have proposed a model based on the ideas derived from colloid stabilization (Jeon et al. 1991). However, their model is not able to explain the protein resistant nature of the surfaces grafted with shorter oligoethylene glycol chains (consisting 3-6 ethylene glycol subunits) and is, thus, only applicable to surfaces coated with longer PEG molecules. According to the theory,

proteins approaching the PEGylated surface compress the hydrated PEG layer and, as a result, the water molecules residing inside the layer are forced out. The removal of the water is thermodynamically unfavorable and, hence, contributes to the steric repulsion effect and the inertness of the PEGylated surfaces. Water content in the interfacial PEG layer, i.e. the hydration state, is furthermore considered significant, since high water content contributes to the steric repulsivity of the surface and also indicates a lack of strong attractive van der Waals protein-coating interactions (Malmsten et al. 1998). Accordingly, the theory of Andrade and de Gennes predicts that increased PEG length and surface density along with the increasing water content will result in improved protein adsorption resistance and surface inertness, with the attainment of high surface density being more significant factor than long chain length. The significance of the density and long chain length is furthermore confirmed by the single-chain mean field (SCMF) theory used by Szleizer (1997) that is also able to rationalize the inertness of the surfaces with high density of short PEG chains (<7 subunits).

In addition, somewhat different reasons for the biofouling resistance of polymer grafted surfaces are offered by Besseling (1997) and Grunze (Wang et al. 1997): Besseling was one of the first to propose that the chemical properties of surfaces may have an effect on the state of hydration of the surfaces and on the repulsive or attractive forces that result from the interaction between two surfaces. According to Besseling's theory, which is a generalization of a lattice fluid theory of water, the type of the interaction between surfaces, repulsive or attractive, is determined by the tendency of the surfaces to affect the orientation of the adjoining water layer compared to the bulk water. If a surface predominantly influence the local density of water but not the local orientation of the water molecules, the resulting force between two such surfaces is attractive. This holds true for surfaces with both a high and a low affinity for water. But then again, if the main effect of the surface is to influence the orientational distribution of the nearby water, the ensuing force will be repulsive. This repulsiveness is accounted to be a consequence of the disrupted hydrogen bonding in the hydration layer.

In accordance with Besseling, Grunze's theory relies also on the interaction of the water with the surface polymer layers and highlights the importance of water molecules in creating the antifouling surfaces. Grunze suggests that the polymer chains on the surfaces, when in appropriate conformations, provide nucleation points for water

and, thus, stabilize it. Therefore, the antifouling properties of the surfaces would primarily be accounted to stem from a hydrogel-like, interfacial organized layer of water, that prevent the direct interactions between the proteins and the surface, instead of steric repulsions caused by the polymer chains. The relationship between PEG chain conformations and surface inertness has also been shown to be valid by Harder et al. (1998) who investigated the adsorption of fibrinogen onto oligo(ethylene glycol) (OEG)-terminated self-assembled monolayers (SAM) on gold and silver surfaces. Due to the different lateral densities of the SAMs on the above mentioned surfaces, the conformation of the OEGs was different and, thus, it was shown that the predominantly crystalline helical and amorphous conformations found on gold surfaces produced inert surfaces, whereas all-trans conformations observed on silver surfaces failed to prevent protein adsorption.

2.4.2 Kinetic and thermodynamic prevention of protein adsorption on polymer grafted surfaces

Antifouling properties of surfaces and the prevention of e.g. protein adsorption can be inspected from either kinetic or thermodynamic point of view (Carignano and Szleifer 2000; Satulovsky et al. 1999). Kinetic prevention, concisely, means the ability of the surface to delay the attachment of undesirable particles. Depending on the case, the effective timescale of kinetic prevention varies from a few hours up to a couple of days until it becomes overwhelmed. Therefore its suitability, for instance, in the case of medical implants or artificial organs is questionable, since the implants are integrated into tissues for years. Thus, thermodynamic adsorption prevention, which is rather time-independent, would be more suitable. Thermodynamic prevention refers to the fact that the chemical equilibrium structure of the material surface prefers the state in which there are no adsorbed proteins on the surface (Carignano and Szleifer 2000).

Whether the modified surface is kinetically or thermodynamically antifouling, is determined primarily by the type of interaction between the grafted polymers chains and the surface itself. The most suitable surface modifiers when considering kinetic prevention, are polymers that are not attracted to the sorbent surface. Subsequently, the polymers that have high affinity to the surface, are best suited for thermodynamical prevention. In both cases, high polymer density is desirable. For thermodynamic control there are two major contributing factors. Firstly, since the polymers are attracted to the

surface, a high local concentration of the polymers exists near the surface. This causes a strong steric repulsion on the approaching proteins close to the surface. Secondly, the polymers and the proteins compete for the same adsorption sites on the surface, therefore, making the adsorption of the proteins more difficult. For kinetic prevention, on the other hand, the main mechanism relies on the dense forest of polymer chains that protrude out of the surface and create an effective long-range steric barrier (Carignano and Szleifer 2000; Satulovsky et al. 1999).

2.4.3 Rigid or flexible chains

Based on molecular mean-field theory calculations Carignano and Szleifer (2000) confirmed the general belief that flexible, surface-tethered polymers are more effective at preventing protein adsorption than rigid polymer chains. They also investigated whether the extensibility of rigid polymer chains could be used to promote the expression of surface bound ligands to enhance specific protein or cell interactions. According to them, the rigid chains have much weaker ability to prevent protein adsorption on the surface even though the kinetic barrier consisting of rigid chains reaches much further into the surroundings than in the case of flexible polymers. Thus, for rigid chains the range of repulsion is longer. Nonetheless, as a whole, the barrier created by rigid chains is weaker and, hence, in terms of kinetic control flexible chains appear to be more potential in preventing protein adsorption. Additionally, thermodynamically speaking the difference seems to be rather obvious. For optimal control, the attraction between surface and polymers is required to eliminate the protein adsorption through overwhelming competition over binding sites. Rigid polymers only have limited probability to be at different angles with respect to the surface, whereas flexible polymers can bend and organize themselves endlessly. Hence, much more effective surface attraction and, consequently, protein repulsion is attained with flexible chains. Nevertheless, based on the longer extensibility of rigid chains and more constrained structure, rigid polymers could be used to attune the accessibility of surface bound ligands and even guide the protein adsorption both spatially and conformationally, if suitable mixtures of flexible and rigid chains were to be used.

However, the above mentioned results are based on theoretical calculations and, for example, Kane et al. (2003) have suggested that the antifouling properties of PEGylated surfaces rely on the kosmotropicity, i.e. the ability of PEGs to stabilize and

organize water-water interactions and, thus, simultaneously as a sort of a byproduct stabilize macromolecular structures as well, preventing their structural alterations upon surface contact and consequently their adsorption. Indeed Kane et al. (2003) pointed out that while the structural and conformational flexibility may contribute to the antifouling properties of the PEGylated surfaces, it is, however, not a prerequisite for neither kosmotropicity nor even required for protein resistance of surfaces. As a supporting evidence, SAMs of conformationally very constrained piperazine derivatives and relatively stiff sarcosine derivative polymers have been observed to be able to resist protein adsorption (Ostuni et al. 2001). Although nonetheless, it is admitted by Kane et al. (2003) and Ostuni et al. (2001) that in some situations the flexibility may be an extremely significant factor in determining the antifouling properties.

2.4.4 Testing of the antifouling properties of polymer grafted surfaces

The resistance of surfaces against biofouling is typically measured with short-term adhesion tests where the surfaces are exposed to either proteins or bacterial cells for a couple of hours at static conditions. The amount of biofouling is then typically quantitated through the changes in fluorescent dye intensity on the surface or as accurate amount of cells or colonies. In general, it is a very widespread mindset in biofouling literature and research that by interfering and preventing the initial adhesion of proteins and bacteria to surfaces the subsequent formation of biofilms and aggregation of harmful material could be prevented (for example Miller et al. 2012; Zhang et al. 1998; Yang et al. 2011). However, it has been claimed that studies relying only on short timescales may not be reliably used to evaluate the long-term biofouling tendencies of surfaces, and that the results of long- and short-term experiments may result in completely different conclusions. For, instance, Miller et al. (2012) showed that while polydopamine and polydopamine-g-poly(ethylene glycol) coated ultra- and nanofiltaration membranes expressed clear reduction of bovine serum albumin protein and *Pseudomonas aeruginosa* adhesion in short-term biofouling tests, all of the modified surfaces failed to prevent biofouling and biomass accumulation in longer 10-day experiments. Additionally, they pointed out that in actual, e.g. industrial, settings the biofouling is typically a cooperative series of events including various types of bacteria and biological substances and, hence, experiments with single model organism or protein may not provide completely reliable information. Also in terms of bacterial

biofilms, different kinds of bacteria may benefit synergistically from each other and some strains isolated from the biofilms may not even be able to produce biofilms by themselves when grown in a pure culture (Tang et al. 2009). Thus as a conclusion, short-term batch adhesion tests with model molecules or cells ought not to be directly considered as a measure of antifouling tendency but instead as a guidelines that require further assurance from other more comprehensive and pragmatic tests (Miller et al. 2012). Thus, in addition to short-term tests other indicators and experimental setups ought to be considered and developed to fully evaluate the antifouling properties of surfaces.

2.5. Bacterial adhesion to polymer coated surfaces

Generally the primary effector behind bacterial adhesion to surfaces is considered to be the recognition of adsorbed organic material on the target surface by the bacteria. This recognition event may be specific or non-specific but in any case the most important material to be recognized is suggested to be of proteinaceous origin (Wei et al. 2003). However, biofouling experiments with polymer tethered surfaces and bacterial cells have revealed that in some occasions bacterial attachment and possible later biofilm formation is possible even without initial protein adsorption or the presence of the proteins on the surface (Gon et al. 2012; Wei et al. 2003). Hence, despite the general trend, the ability of surfaces to resist protein adhesion does not necessarily correlate with their tendency to prevent bacterial accumulation.

Due to the relatively large size of the bacterial cells as compared to proteins, the bacteria cannot readily infiltrate themselves into the polymer tethered surfaces to facilitate adhesion. Instead the ability of bacteria to cling on a coated surface is dependent on specific adhesion points on the surface, e.g. flaws in the coating layer complemented with, among others, suitable surface characteristics or electrostatic hotspots, which allow them to attach tightly and overcome the steric repulsions caused by the polymer layer (Gon et al. 2012). Thus, the antifouling polymer barrier is not bypassed but rather becomes compressed under the bacteria. Therefore, the effectivity of bacterial repulsion is mostly dependent on the content or the total mass of the tethered polymers on the surface and, consequently, somewhat independent on tether length and spacing, within reasonable parameters.

Interestingly, since bacteria are much larger than proteins they also seem to be more sensitive to take advantage of minor flaws in surface polymer coatings and, as a result, are more eager to attach on slightly damaged surfaces. Because of their broader dimensions bacteria are more able to multivalently bind, i.e. attach to many minor surface defects simultaneously, which strengthens their adhesivity, whereas smaller proteins are not able to implement multivalent binding unless the surface defects are closely situated. Proteins also exhibit more pronounced sensitivity to polymer brush architecture due to their tendency to penetrate into the polymer layer, whereas bacteria are mostly concerned about compression characteristics of the polymer brushes (Gon et al. 2012).

2.5.1 Bacteria floating in suspension may attach to solid surfaces and form biofilms

Biofilms consist of populations of micro-organisms that are concentrated typically at solid-liquid interface. These organisms are further encapsulated by extracellular polymeric substance (EPS) produced by the bacteria themselves and this slime is primarily responsible for the overall biofilm structure (Stoodley et al. 2002). Biofilm enhances the survival and growth of the bacteria living inside it, but at the same time biofilms are extremely harmful from the point of view of efficacy, utility or hygiene of, for example, industrial and healthcare-related equipment (Hall-Stoodley et al. 2004).

Active bacteria can adhere to almost any surface and biofilms provide obvious benefits when comparing to free-growing and swimming bacteria in suspension. First of all, surfaces provide solid and reasonably stable space and environment for the bacteria to thrive and proliferate. Also, by bringing cells close to each other and to the surfaces biofilms may have kind of catalytic functions as the confined localization facilitates communication and cooperativity between the cells inside the biofilm. Secondly, biofilms protect bacteria from a myriad of various otherwise noxious environmental challenges, such as UV light, salinity and dehydration, metal toxicity, antibiotics and other antimicrobial agents and phagocytosis (Dibdin et al. 1996; Espeland and Wetzel 2001; Leid et al. 2002; Le Magrex-Debar et al. 2000; Teitzel and Parsek 2003). Thirdly, bacterial evolution has also been observed to be enhanced within biofilms, due to increased gene transfer potential. Plasmids are readily dispersed via conjugation in dense bacterial populations and, additionally, DNA release and subsequent

transformation are found to be common inside biofilms (Molin and Tolker-Nielsen 2003).

2.5.1.1 Antibiotic resistance of biofilms

Three different mechanisms are thought to contribute to the resistance of biofilms to biocidal agents. The EPS, i.e. the slimy matrix of the biofilm, is considered as the first one, since it may function as a barrier and, thus, prevent the entrance of the harmful substances inside the biofilms, neutralize them or at least dilute them to sublethal concentrations before the bacteria inside the biofilms become morbidly affected (Dibdin et al. 1996; Mah and O'Toole 2001). The second stage of defense is thought to be dependent on the physiological state of the cells in the biofilms. Oftentimes biofilms include organisms in stationary or dormant states where they are insensitive especially to antibiotics that interfere with metabolic pathways. Therefore, the existence populations of stagnant bacteria inside biofilms seems to be a rather significant contributor to the observed biocide resistance (Anderl et al. 2003; Walters et al. 2003). Third possible mechanism is suggested to be the existence of some bacterial subpopulations in the biofilms that are resistant to e.g. certain antibiotics. These cells are more likely to survive antimicrobial attacks and continue to proliferate even though their numbers in the total biomass of the biofilm would be seemingly insignificant (Spoering and Lewis 2001). However, whether these cells actually represent an actual distinct phenotype or are just the toughest and the most resilient individuals within the biofilm's population distribution, remains to be discovered (Mah and O'Toole 2001).

2.5.1.2 Stages of biofilm formation

Biofilm formation comprises of a series of events that can be divided into five different phases (Stoodley et al. 2002). The first stage comprehends the establishment of the conditioning layer that consists of organic and inorganic molecular sorbents that adhere on the surface and initial attachment of cells. Following the attachment, the bacteria produce EPS which enables the initial adhesions to become stronger and thereby allows the biofilm formation to proceed. At the third stage the attachment is further strengthened as the sessile bacteria proliferate and the colonies begin to spread out on the surface and simultaneously facilitate the localization and colonization of other bacteria as well (Klausen et al. 2003; Stoodley et al. 2002). Overall the adhesion

becomes more robust and cells begin to aggregate and organized structures start to emerge and become more evident (Stoodley et al. 2002). At the fourth stage the biofilm continues to mature and organize itself and it is e.g. remarkably able to disturb the functionality of a filter membranes onto which it has grown (Flemming and Schaule 1988; Stoodley et al. 2002). Interestingly, the ultimate shape of the biofilm seems to be greatly determined by the available nutrient source, and depending on the environment the film may appear, for instance, flat or mushroom shaped (Klausen et al. 2003). The final stage of the biofilm formation is considered to be achieved when the bacteria in the biofilm return to transient motility stage and, as a result, the cells can be shed from the biofilm and they become able to migrate to new sites away from the biofilm (Stoodley et al. 2002).

3 Main goals of the thesis

The primary goal of this thesis was to produce stainless steel (SS) surfaces coated with silane-PEG layer to investigate if the silane-PEGs are suitable for modifying the SS surfaces and how well the the characteristics of the SS can be modified with the silane-PEG coating. The actual surface physicochemical properties were studied with specific surface sensitive methods, whereas the functionality of the modifications, i.e. the antifouling potential caused by the silane-PEGs, was assessed with exposure tests with bacterial cells or protein solutions. Additionally, further surface modifiability was examined by testing if avidin molecules could be added to coatings prepared by using biotin-terminated silane-PEG.

The general workflow of the thesis was as follows: Firstly, the silanization protocol was tested and the modification process itself was confirmed to be reliable and replicable. Secondly, the modified surfaces were analyzed and characterized with X-ray photoelectron spectroscopy (XPS) and contact angle measurements to assess the quality of the coatings. Thirdly, the biofouling resistance of the modified surfaces was tested with bacterial and protein adhesion tests and, finally, specific surface functionalization potential was tested utilizing avidin-biotin -coupling.

Together these experiments should provide a useful overview with a basic set of tools considering the modifiability of SS surfaces with silane-PEG derivatives. Naturally, insights about surface modifications in general were also gathered and a foundation laid for the possible future investigations and practical applications as well as further development of the tested surface modification methods.

4 Materials and methods

4.1 Stainless steel surface modification

4.1.1 Stainless steel samples

12.5 x 28 x 0.7 mm stainless steel (SS) chips (AISI 316L) were used as substrates (Figure 1). The chips were ordered from Outokumpu Stainless Oy (Finland). The samples were laser-cut but, however, still partly attached to larger SS sheets. Thus, each of the individual SS chip to be used was cut from the sheet with diagonal cutters and the possible rough edges were smoothened with a diamond file prior to any treatments. The chips were labeled with running numbering for identification purposes. The numbers were carved onto the backsides of the samples.

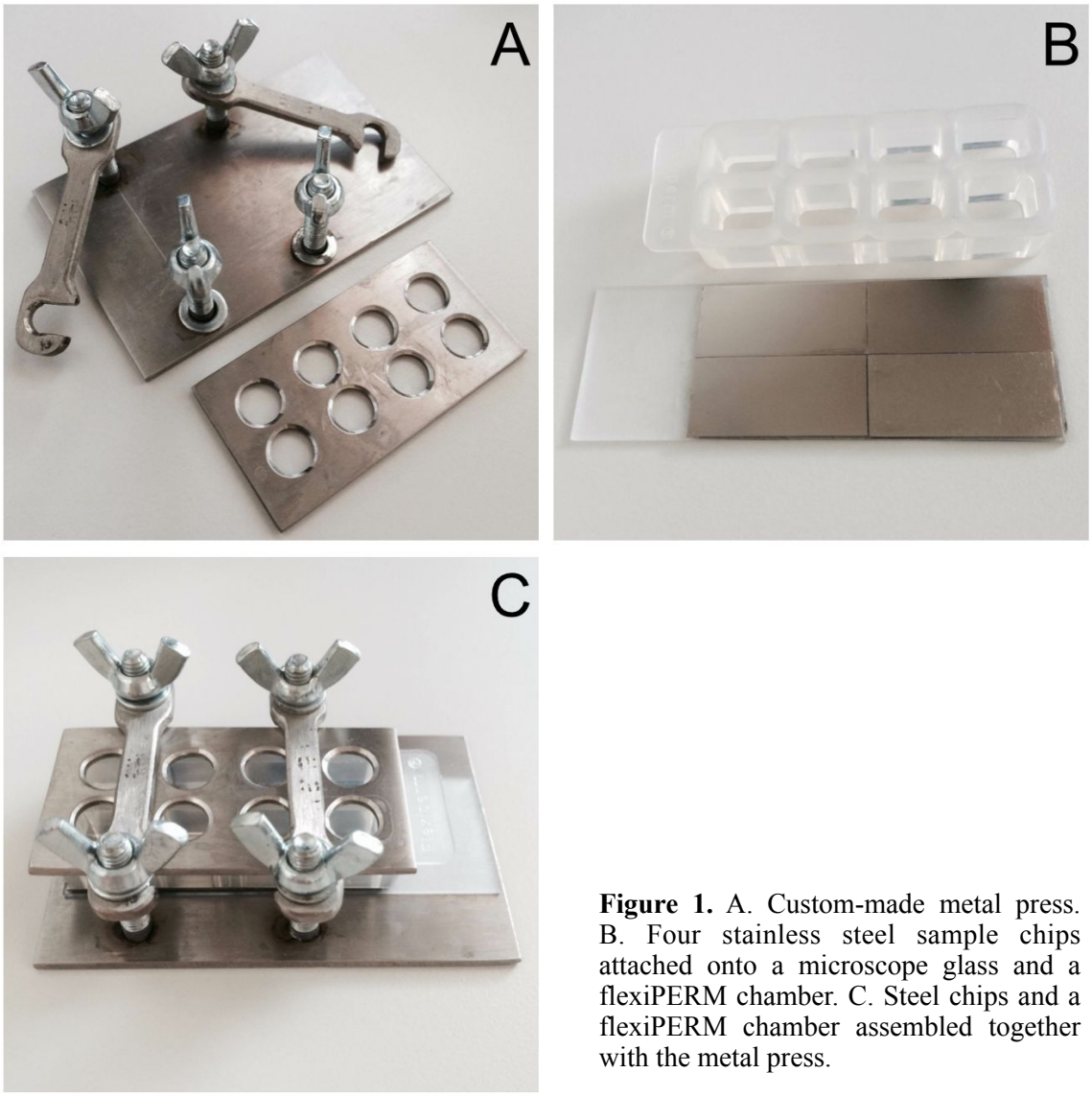

Figure 1. A. Custom-made metal press. B. Four stainless steel sample chips attached onto a microscope glass and a flexiPERM chamber. C. Steel chips and a flexiPERM chamber assembled together with the metal press.

4.1.2 Silane-polyethylene glycol molecules

Silane-polyethylene glycol derivatives (silane-PEGs) of molecular weight of 2 kDA with carboxylic acid (silane-PEG-COOH, SPC) or biotin (silane-PEG-biotin, SPB) head groups were used. All silane-PEGs were obtained from Nanocs (USA) ad used as received. The silane-PEGs were stored protected from light and moisture at - 20 ºC.

4.1.3 Silanization

Prior to any experiments, the SS substrates were washed by sonicating them in absolute ethanol and in deionized water for 10 minutes each. For passivation a customized three-electrode electrochemical cell was used together with Autolab PGSTAT12 potentiostat/ galvanostat (Methrom Autolab) and Nova 1.5 software (Hannula 2012). An Ag/AgCl electrode (Methrom Autolab 3.109.0830) was used as a reference electrode and 0.1 M H_2SO_4 as electrolyte solution. The solution was changed for a fresh one after every two samples. The fresh solution was degassed before passivation procedure by bubbling with N_2 for one hour and then for 10 minutes between the samples. Moderate degassing was also continued throughout the passivation. At first the SS chips were reduced for 10 minutes with the current of 5 mA/cm^2 and then passivated with the constant voltage of 0.2 V for another 10 minutes. After the passivation the samples were rinsed with deionized water and dried under N_2 gas stream.

For silanization silane-PEGs with either COOH or biotin end group were solubilized in toluene to desired concentrations (3 or 5 mg/ml). Mixture was vigorously shaked for 30 minutes or until the silane-PEGs were completely solubilized. The SS samples were placed into glass vials, immersed into the silanization solution and then incubated on a rocking shaker for approximately 20 h (over night) or for 41-45 hours (over two nights). After the incubation the SS samples were washed twice with a pressured stream of toluene from a pipette followed by immersion in toluene for 30 s and then three times with a stream of water followed by immersion in water for 30 s with vigorous shaking. The samples were air dried under a laminar flow. Some samples were also additionally heated for 10 min at 100-105 °C after the silanization to enhance the possible covalent coupling between the silanes and SS surface.

4.2 Surface characterization

4.2.1 X-ray photoelectron spectroscopy

X-ray photoelectron spectroscopy (XPS) measurements were performed in the Surface science lab lead by Professor Mika Valden in the Department of Physics at the Technical University of Tampere by using Multilab equipment (Lahtonen et al. 2006). SS chips silanized with both 3 and 5 mg/ml silanization solutions of silane-PEG-COOH with silanization time of 2 days were measured, and electrochemically passivated, uncoated SS surface was used as reference. The passivation of the control sample was performed just prior to the measurements. Non-monochromatized Al Kα X-rays (1486.6 eV) were used for excitation and the measurements were carried out in normal emission with a detection area of ~600 um in diameter. The surface elemental concentrations and chemical states of compounds were identified by analyzing the high-resolution spectra of C 1s, O 1s, Si 2p and S 2p. Also the depth and coverage of the silane-PEG coating was determined. Both 0° and 60° measurement angles were used. After subtracting a Shirley-type background, the spectral components were fitted with a combination of Gaussian and Lorentzian line shapes. CasaXPS and QUASES-Tougaard softwares were used for spectral analysis. The data analysis was performed by doctoral students Markku Hannula and Elina Lehtonen.

4.2.2 Atomic force microscopy

Atomic force microscopy (AFM) measurements were performed in the Nanoscience center at the University of Jyväskylä by doctoral student Kosti Tapio from the Molecular Electronics and Plasmonics group led by Docent Dr. Jussi Toppari. Dimension 3100 (Bruker) atomic force microscope was used together with Nanoscope Analysis software (Bruker) and Aspire CT300 Conical tapping mode AFM probes (Part No. CT300R-25, nanoScience Instruments). Height, amplitude and phase images were recorded using tapping mode and images of the size of 1 x 1 μm, 3 x 3 μm and 10 x 10 μm were taken from each sample. SS samples silanized with 3 and 5 mg/ml silane-PEG-COOH and silane-PEG-biotin solutions with a silanization time of 2 days were analyzed. Also SS-silane-PEG-biotin surfaces functionalized with wildtype avidins (Belovo, Belgium) were imaged.

The samples that were to be functionalized with avidins were immersed in 3 μg/ml solution of avidins in PBS for 1.5 hours after the silanization. They were then

washed six times with PBS + 0.05% Tween20 and once with PBS for 30 s under shaking each time and finally rinsed with water. The samples were air dried under laminar flow and sealed into plastic centrifuge tubes. Clean SS chips that were washed by sonicating as described in "Silanization" and silane-PEG-biotin coated samples without avidin functionalization were used as controls. All samples were prepared at BioMediTech at the University of Tampere and thereafter delivered to Jyväskylä. Doctoral student Kosti Tapio performed the imaging.

4.2.3 Contact angle measurements

Contact angle measurements were conducted at the Department of Material Science at the Technical University of Tampere (TUT). Custom made imaging system together with Pisara drop image analyzing software (FotoComp, Finland) was used. Drops of 4 µl of water were used for measurements, 7-12 drops per each SS chip. Images were taken immediately after adding the drops on the surfaces. Contact angles were measured from the surfaces of SS chips with silane-PEG-COOH and silane-PEG-biotin coatings (3 mg/ml silanization solutions and a 2-day silanization time used in both cases). Silanization was done as described in section "Silanization" and the protocol was used with and without the additional heating step for both kind of samples. Clean uncoated SS chips that had been washed by sonicating as described in "Silanization" were used as reference.

4.2.4 Scanning electron microscopy

Scanning electron microscopy (SEM) was performed by doctoral student Tommi Isoniemi in the Department of Physics at the University of Jyväskylä. The samples were prepared at BioMediTech at the University of Tampere and then sent to Jyväskylä. Silane-PEG-COOH coated SS chips with a 2-day silanization time as well as clean SS chips without silane coating were made. Some of the samples were also exposed to bacteria and had the cells fixed onto them before imaging as depicted in "*E. coli* adhesion test" to provide a closer look at the bacterial adhesion on the surfaces.

4.3 Adhesion tests and avidin functionalization

4.3.1 Protein adsorption test

The SS chips were silanized with silane-PEG-COOH as described in section "Silanization". 3 mg/ml silanization solution and 2 d incubation time was used.

Reference SS chips were only washed by sonicating them in ethanol and water for 10 minutes each and dried with N_2 stream. The chips were attached onto microscope slides with double-sided adhesive tape (Scotch) and flexiPERM micro12 chambers (Sarstedt) were placed thereupon and secured in place with self-made metal presses (Figure 1). 3 and 30 µg/ml solutions of both wildtype chicken avidin (Belovo, Belgium; M = 16 kDa/monomer) and fibronectin (gelatin-affinity purified from human serum; M = 440 kDa/monomer) were prepared. The proteins had been labeled with Alexa 488 fluorescent dye by Dr. Jenita Pärssinen and were solubilized in phosphate buffered saline (PBS). The labeling ratio for avidin was 0.47 and for fibronectin 8.1 moles of dye per one mole of protein. For the avidin solution this equals 29.38 µmol of dye per 1 g of protein and for the fibronectin solution 18.41 µmol of dye per 1 g of protein. The protein solutions were applied on the SS chips in flexiPERM wells and incubated for either 1 or 3 hours protected from light at room temperature. Pure PBS was added into control wells for 3 hours instead of protein solutions. The samples were then washed three times with PBS, flexiPERM chambers removed and the chips allowed to air dry. Coverslips were mounted onto the SS chips using HardSet mounting reagent (Vectashield, Cat. No. H-1400). The ready-made samples were stored shielded from light at +4 ºC.

The samples were imaged using Zeiss LSM-780 confocal microscope with Zen Black software. 10 images were taken from each flexiPERM well area at random locations: 5 images were taken with 10x objective and 5 images with 20x objective from each flexiPERM well. 488 laser with fixed settings was used for every image (gain: 760; digital offset: 0; digital gain: 1). Mean intensities of the pictures, as given by Zen Black software, were recorded and used as measurement of the amount of adsorbed protein on the surfaces.

4.3.2 *E. coli* adhesion test

E. coli Top10 cells were used for studying the bacterial adhesion. One bacterial colony from an agar plate was inoculated into a 50 ml centrifuge tube with 20 ml of LB medium and precultured overnight at + 37 ºC on a platform shaker at 150 rpm. Optical density (OD_{600}) of the preculture solution was measured at 600 nm and adjusted to 2.0 if needed. To adjust the OD, the culture was diluted with LB or centrifuged for 10 minutes at 3500 rpm followed by resuspension of the pellet into suitable amount of LB.

The SS chips were silanized with silane-PEG-COOH or silane-PEG-biotin as described in section ”Silanization”. 3 and 5 mg/ml silanization solutions and 1 and 2 days silanization times were used. Uncoated reference SS chips were washed by sonicating in ethanol and water for 10 minutes each and dried with N_2 stream. The chips were placed in the wells of a 6-well plate and 2 ml of bacterial suspension was added to each well. The samples were incubated on a rocking shaker for 1 hour at room temperature. Suspension was aspirated and the SS chips washed twice with water by shaking for 30 s. The samples were air dried under a laminar flow and the attached bacteria were then fixed and stained by immersing the samples into a solution of 3 mg/ml of acridine orange in 2% glacial acetic acid for 2 minutes protected from light. The staining solution was aspirated and the samples washed twice extensively with water by shaking for 30 s and then allowed to air dry under laminar flow. The chips were attached onto microscope glasses with double-sided adhesive tape (Scotch) and covered with coverslips using HardSet mounting medium (Vectashield Cat. No. H-1400). The ready-made samples were stored shielded from light at +4 ºC.

The samples were imaged using either Zeiss LSM-780 confocal microscope with Zen Black software or with Zeiss Axio Apotome equipped with an AxioCam MRm camera. With LSM-780 five 10 x 10 mosaic images were taken from each SS chip with 63x oil immersion objective whereas with Apotome 10 snap shots per sample, also with 63x oil immersion objective, were taken. To make sure the LSM-780 mosaic pictures stayed in focus, they were captured as Z-stacks and then converted into a maximum intensity projection image to obtain a single layered image. All pictures were taken from random locations on the chips. The bacteria visible in the pictures were calculated with ImageJ either semi-automatically using the Analyse particles and Treshold operations together with background reductions and contrast adjustments if necessary or by hand using the Cell Counter tool in the case of bad quality images or if the cells were so few and far between that they could easily be manually calculated.

4.3.3 Avidin functionalization of silane-PEG-biotin surface

The SS substrates were prepared as described in ”Silanization”. 3 mg/ml silane-PEG-biotin solution was used and the samples were immersed in the solution over two nights. Steel samples with silane-PEG-COOH coating (3 mg/ml silanization solution with 2d silanization) were also made to be used as negative controls. For biotin detection

streptavidin-alkaline phosphatase (SA-AP)(Roche Diagnostics, Product No. 11093266910) was diluted in 1:5000 ratio in Tris buffer (100 mM Tris-HCl, 150 mM NaCl, pH 7.5). In addition, biotin-blocked SA-AP in Tris buffer was prepared as another negative control: First 2 µl of SA-AP was incubated over night with 9.6 µl of biotin (c=700 µM) and the mixture was then diluted 1:5000 in Tris buffer. 600 µl of SA-AP solution with either biotin-blocked or unblocked SA-AP was then applied onto each coated steel sample. SS surfaces with silane-PEG-biotin coating together with SA-AP solution were the actual samples, whereas silane-PEG-biotin coated surfaces with biotin-blocked SA-AP and silane-PEG-COOH coated surfaces with unblocked SA-AP were used as controls. Samples were incubated for one hour at room temperature and thereafter washed six times by shaking for 30 s with PBS-0.05% Tween 20. A drop of 40 µl of p-nitrophenyl phosphate substrate (pNPP, 1 mg/ml of pNPP in 1 M diethanolamine + 0.5 mM $MgCl_2$, pH 9.8; stored in the dark at +4 ºC) for SA-AP was then applied on each SS chip and the chips were covered with aluminum foil to protect them from light. 2 µl samples were pipetted off from the drops at time the points of 10, 20, 30, 40, 60 and 120 minutes and their absorbances were measured with NanoDrop 2000 (Thermo Scientific) spectrophotometer at 405 nm. NanoDrop was blanked before each sample with 1 mg/ml of pNPP in 1 M diethanolamine with 0.5 mM $MgCl_2$ (pH 9.8).

5 Results

5.1 Surface characterization

5.1.1 X-ray photoelectron spectroscopy

XPS analysis showed that silane-PEGs indeed attached onto the SS surfaces and form thin but nonetheless rather uniform and extensive coating. This was confirmed by the increased signal of the C-O component of carbon and oxygen, arising from PEG chains, as well as the existence of Si 2p signal, that originates from the Si atom of the silane-PEGs, recorded from all samples except for clean SS controls (Figure 2). However, according to the Si-O signal of oxygen spectrum, siloxane bonds between silane molecules themselves (Si-O-Si bonds) and between silane-PEGs and the SS surface (Si-O-Metal bonds) were scarce and, thus, the silane-PEGs do not seem to be able to form distinctive siloxane network onto the SS surface as is known to happen, for example, in the case of smaller (3-aminopropyl)trimethoxysilanes (APS) (Jussila et al. 2010). Therefore, it is possible that the silane-PEGs were attached onto the SS surface via physisorption instead of covalent siloxane bonding. Overall there appeared to be no significant differences between the qualities of the silanized SS samples, and the chemical compositions and states of the silanized surfaces were rather identical regardless of the concentration of the used silanization solution (3 or 5 mg/ml). However, the thickness of the obtained silane coatings differed between 3 and 5 mg/ml samples since the average thickness of the silane-PEG coatings was 4.7 Å for the 3 mg/ml samples and 7.35 Å for the 5 mg/ml samples. Nonetheless, the coverage of the SS surface by the uniform silane-PEG coating was observed to be rather extensive and not dependent on the concentration of the silanization solution used. The surfaces were measured to be completely covered and approximately 86 percent of the coverage was found to be of good and homogenous quality. The rest of the surface was expected to be covered with silane-PEG clusters whose thickness exceeded the information depth and, thus, could not be measured. Also some phosphorus was detected in 5 mg/ml silanized samples, but the origins of it is unknown. The error margin for thickness and coverage measurements could be estimated to be 15%.

A

Atomic percentages of chemical states found on silane-PEG-COOH coated and passivated control SS surfaces

	C-C, C-H	C-O	C=O	C=O	Si-O	OH, C-O	Metal-O	Si	S SO_4	S SO_x	P
3 mg/ml SPC	6.90	13.92	6.46	5.59	18.67	21.07	24.81	1.38	1.19	0.00	0.00
5 mg/ml SPC	8.53	10.21	6.58	5.80	18.69	25.86	17.25	3.09	1.51	0.00	2.47
SS control	10.53	5.45	2.47	6.95	27.83	20.58	20.05	2.52	3.62	0.00	0.00
5 mg/ml SPC at 60°	12.29	10.45	7.54	4.79	14.65	30.98	13.56	1.62	1.38	0.18	2.57
SS control at 60°	13.53	4.30	2.31	6.60	29.96*	20.85	17.80	0.00	4.66	0.00	0.00

B

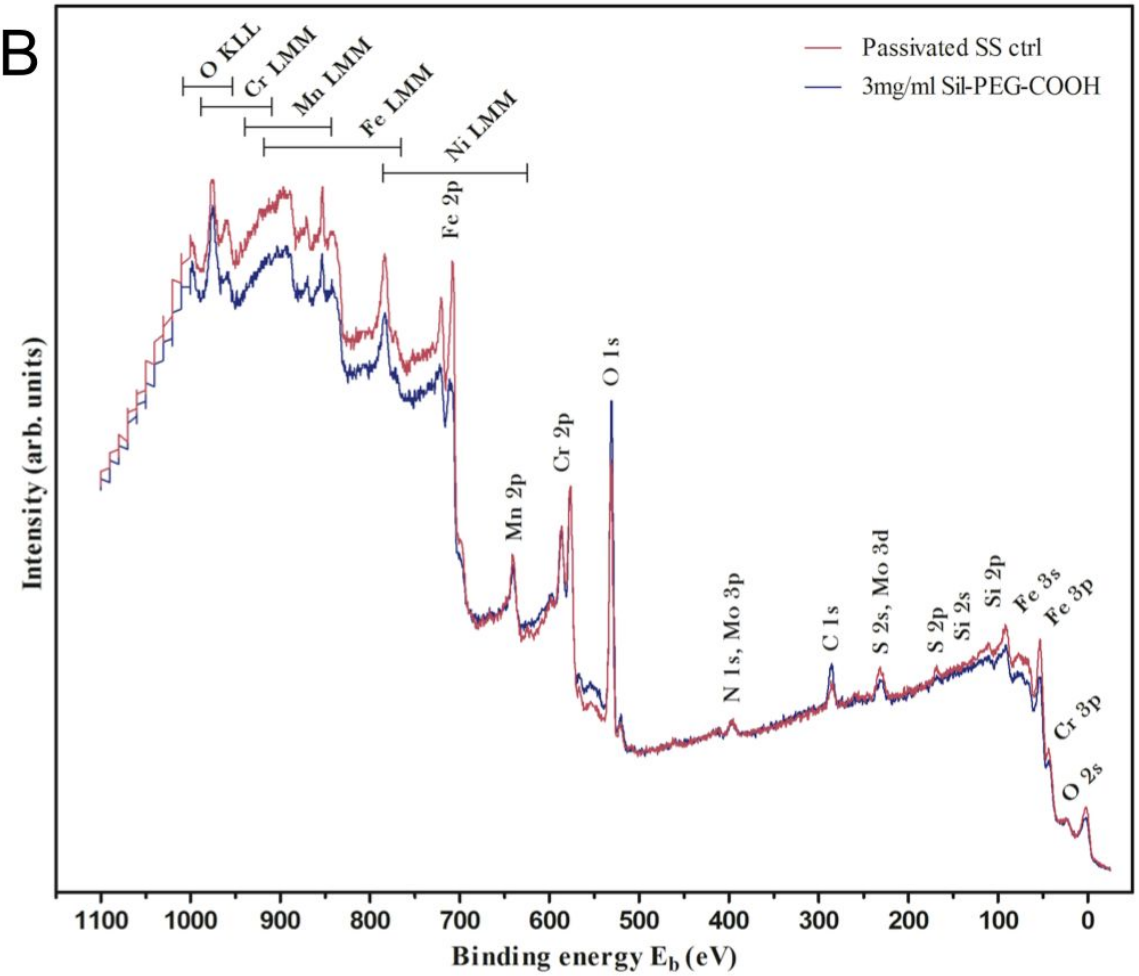

Figure 2. A. Table showing atomic percentages and chemical states of the elements observed on silane-PEG-COOH coated and passivated control stainless steel (SS) surfaces. Silane-PEG-COOH (SPC) samples were covered either 3 mg/ml or 5 mg/ml SPC solutions. Numbers are presented for measurements at 0° measurement angle and for more surface-sensitive 60° measurement angle. The atomic percentages of chemical states are calculated from the spectra of the underlined elements. B. Representative survey scan spectra of silane-PEG-COOH coated and uncoated control steel surfaces. Intensity maximas of observed elements are labeled.

(*) The control samples did not contain siloxane bonds, but the peaks in the 1s spectrum of oxygen and, hence, the calculated atomic percentage of Si-O were a results of presence of sulfate residues on the samples. The peaks of sulfate are observed at the same bond energy as siloxane bonds in XPS measurements.

5.1.2 Atomic force microscopy surface characterization

The silane-PEG coating could not be directly observed with AFM and, hence, the silanized samples looked remarkably similar than the plain SS controls (Figure 3). Grooves and distinctive domain structures of the steel surfaces were apparent in all samples regardless of the silanization. There were also no differences between the height profiles of the controls and the silanized samples. Typically the height of the grooves observed were 2-5 nm for all samples. However, the dips of the grooves were found to vary between coated and non-coated samples. For the uncoated SS controls the groove dip was measured to be from -10° to -20° in 3 x 3 µm images, whereas for the silanized samples the dip was between -2° and -3° (3 mg/ml silane-PEG-COOH coating) and between -1° and -4° (5 mg/ml silane-PEG-COOH coating). Additionally, since phase images express different contrast for different materials, based on the images it could be deduced that at least the grooves on the surfaces contained material other than steel that most likely was silane-PEG. Despite the positive hints, however, AFM was unable to directly and irrefutably detect the silane-PEGs. Also some nanometer-scale objects were detected on the samples that were most likely impurities or dust adsorbed from environment.

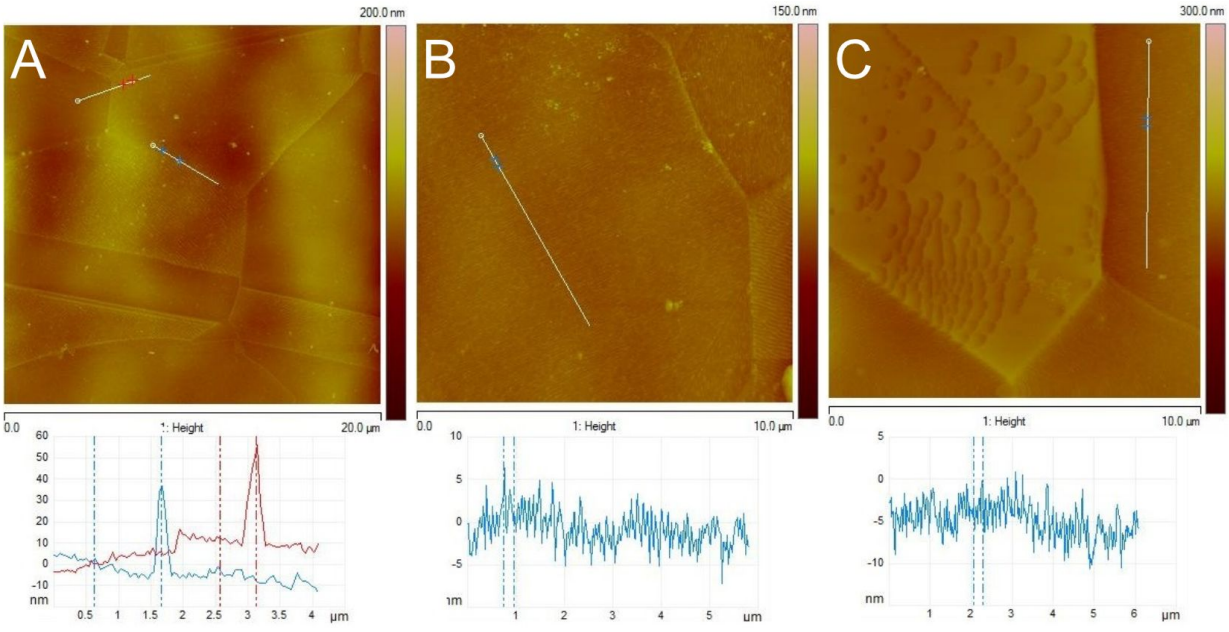

Figure 3. AFM images of silane-PEG-COOH coated and passivated control stainless steel surfaces. A. Clean steel surface, 20 µm x 20 µm dimensions. B. Steel surface coated with 3 mg/ml silane-PEG-COOH coating. C. Steel surface coated with 5 mg/ml silane-PEG-COOH coating. In all images the domain structure of the steel is visible and not blurred by the silane-PEG-COOH coatings. In C some aggregation of the coating is observed. Also cross-section topographies of the surfaces are depicted. The z-axis scale is shown separately in each figure.

5.1.3 Scanning electron microscopy imaging

SEM imaging was performed to visually investigate if the attachment of bacteria on silane-PEG coated steel surfaces differed from the attachment characteristics on clean stainless steel. For example, the effect of anomalies in surface topography and coating quality were assessed in terms of bacterial adhesion behavior. However, the images showed no apparent differences between the silane-PEG-COOH coated samples and control surfaces in terms of the attachment and, in general, the attachment appeared to be rather random (Figure 4). All in all, though, the amount of bacteria on the samples and the overall sample size were rather small which did not allow very comprehensive comparison of the surfaces. Nonetheless, impurities, scratches, silane layer defects or other abnormalities did not seem to have any noticeable effect for the localization or the amount of the attached bacteria. In addition, the natural surface characteristics and structure of SS also appeared not to correlate with the bacterial organization on the surface.

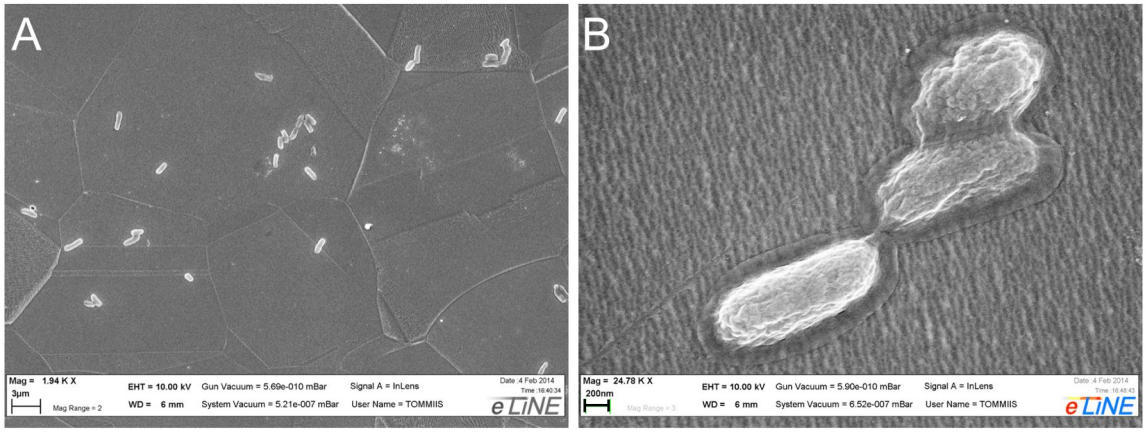

Figure 4. Attachment characteristics of *E. coli* on silane-PEG-COOH coated and uncoated stainless steel surfaces were studied with SEM, but no obvious differences between the surfaces were detected. Moreover, the bacteria were not observed to preferentially bind to e.g. grooves or other defects found on the surfaces. Representative images of *E. coli* bacteria attached on clean stainless steel surface are shown. Scale bar for A. 3 µm and for B. 200 nm.

5.1.4 Contact angle measurements

All silanized samples were found to be more hydrophilic than uncoated SS controls and, in addition, non-heated silanized samples appeared to be more hydrophilic than heated samples. However, statistically significant difference was found only between the heated and non-heated silane-PEG-COOH samples, non-heated silane-PEG-COOH and heated silane-PEG-biotin, uncoated SS controls and non-heated silane-PEG-COOH as well as uncoated SS controls and non-heated silane-PEG-biotin samples (one way

ANOVA with Bonferroni post hoc test, $p<0.05$) (Figure 5). The average contact angle measured for uncoated SS controls was 48.28° ± 6.11° (n = 17). For silanized samples the average angles were as follows: heated 3 mg/ml sil-PEG-COOH sample 43.97° ± 3.67° (n = 28), non-heated 3 mg/ml sil-PEG-COOH 38.57° ± 7.04° (n = 27), heated 3 mg/ml sil-PEG-biotin 45.29° ± 1.70° (n = 11) and non-heated 3 mg/ml sil-PEG-biotin 48.28° ± 6.29° (n = 12).

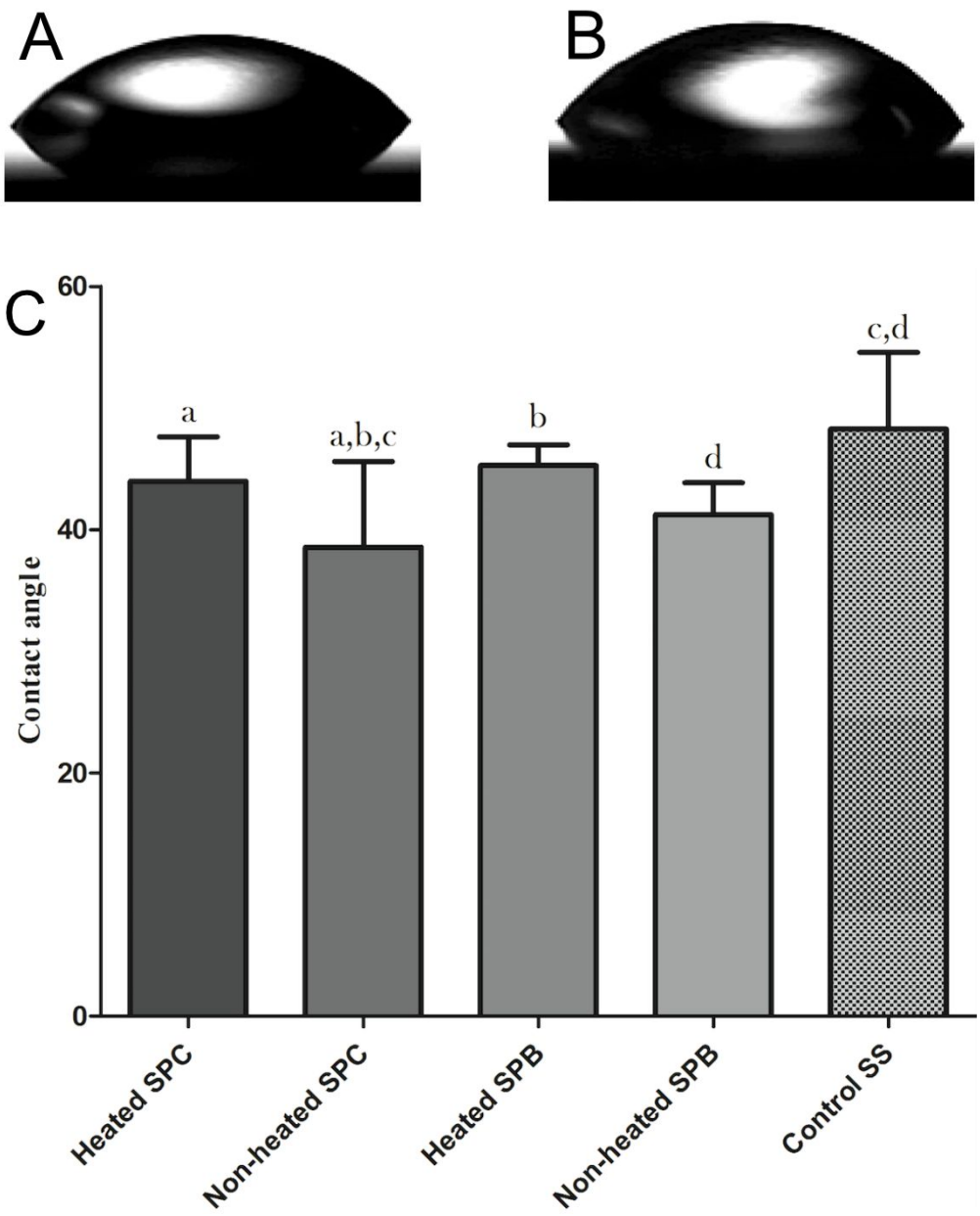

Figure 5. Silane-PEG coating increases the hydrophilicity of stainless steel surface. Representative images of a drop of water on silane-PEG-COOH coated (A) and uncoated (B) stainless steel surfaces are shown. C. Contact angle values of different kinds of surfaces are shown. Average and standard deviation are depicted, and a statistically significant difference exists between the columns labeled with the same letter. The samples were either heated or not during the silanization and coated with silane-PEG-COOH (SPC) or silane-PEG-biotin (SPB). Uncoated stainless steel (SS) surface was used as a reference.

5.2 Adhesion tests

5.2.1 Protein adsorption test

Silanization of SS surfaces remarkably decreased the adsorption of proteins on the surfaces. Based on the fluorescence intensity of the adsorbed protein layer, silanization was found to statistically significantly reduce the attachment of both avidin and fibronectin on SS in all of the tested conditions compared to their respective clean SS controls (One way ANOVA with Bonferroni post hoc test, $p<0.05$) (Figures 6 and 7). In addition, both the increased exposure time and protein concentration positively correlated at least to some extent with the amount of adsorbed protein, since the intensities appeared to be stronger in samples that had experienced the longer incubation time (3 h, labeled as T2) and exposed to the higher protein concentration (30 μg/ml, labeled as C2) (Figure 7). The shorter implemented incubation time (C1) was 1 h and the lower protein concentration (C1) 3 μg/ml. Also at least in this experimental setup, protein concentration seemed to have more pronounced effect on adsorption than exposure time, even though this could not be thoroughly statistically established. C2T1 samples of both fibronectin and avidin on control SS and silanized SS surfaces, nonetheless, showed higher intensities than their respective C1T2 samples. In addition, all of them expressed higher binding than respective C1T1 samples that were subjected to the lower protein concentration for the shorter incubation time. Surprisingly though, the observed mean intensities seemed to stay the same or even decrease when comparing C2T2 samples with corresponding C2T1 samples, hence, supporting the notion of the significance of the higher protein concentration over incubation time.

In general, the observed adsorption patterns of avidin and fibronectin were very similar, although avidin adsorption appeared to have been slightly more efficient. However, the fluorescent labeling ratio slightly favored avidin as the labeling ratio for avidin was 29.38 μmol of dye per 1 g of protein, whereas for fibronectin the ratio was 18.41 μmol of dye per 1 g of protein. In addition, more distinct differences were observed in the organization of the proteins on the SS surfaces. Whereas avidins were more evenly distributed and formed more or less uniform protein layer, fibronectin tended to aggregate and form fibril-like structures, especially with long exposure time and higher concentrations (Figure 6). This is not surprising since fibronectin naturally forms fibers, and the fibers can be readily produced in the absence of cells, for example, by employing water/air interface (Pellenc et al. 2006).

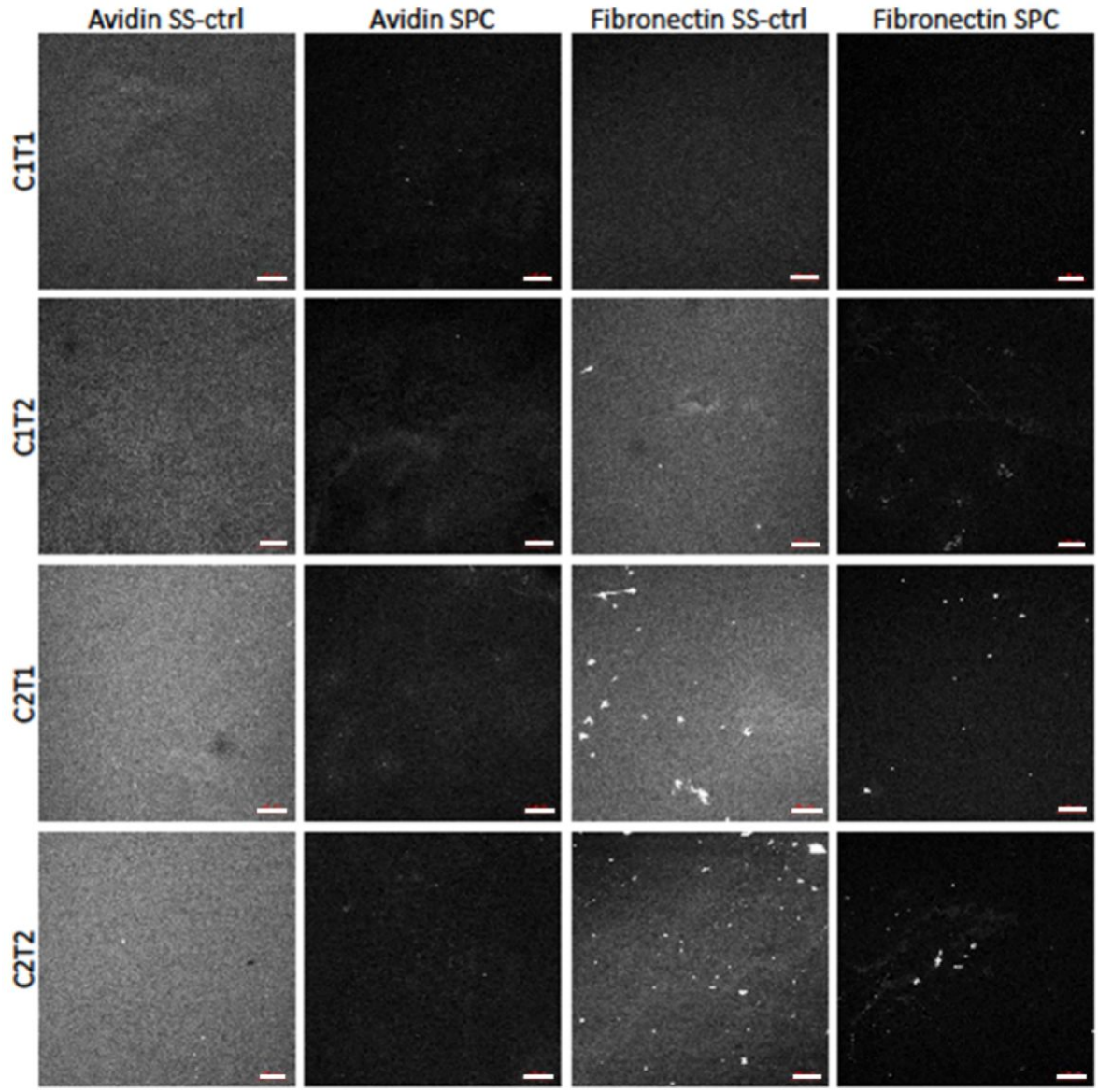

Figure 6. Silane-PEG-COOH coating reduces both avidin and fibronectin adsorption to stainless steel surfaces. Images of fluorescently labeled avidin and fibronectin adsorbed on clean stainless steel surface (SS-ctrl) or on silane-PEG-COOH coated stainless steel (SPC) are shown. Concentration of the used protein solutions was either 3 µg/ml (C1) or 30 µg/ml (C2) and the incubation time either 1 hour (T1) or 3 hours (T2). Fixed microscope settings were used to all images. Scale bar 100 µm.

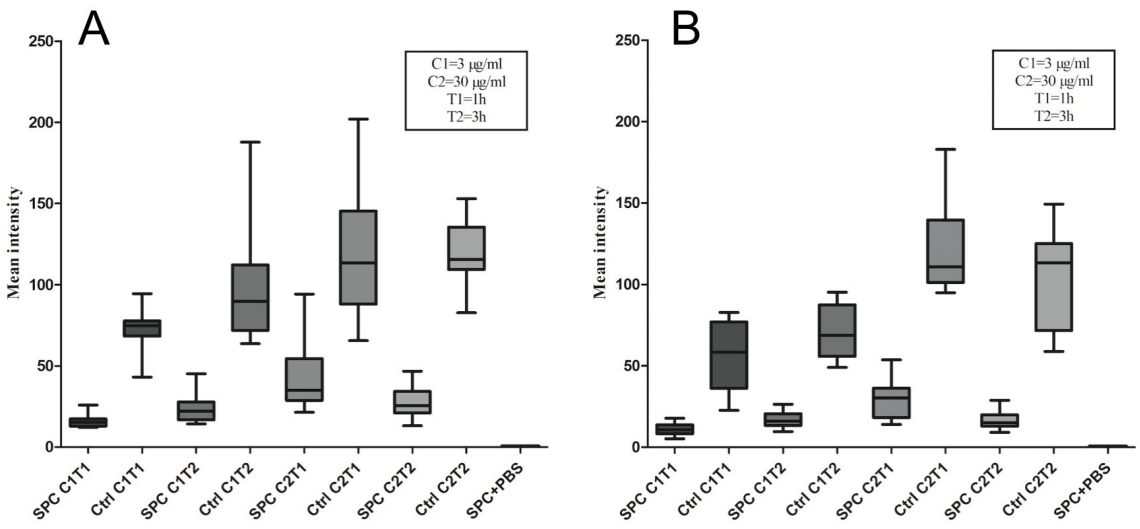

Figure 7. Measured mean fluorescence intensities of avidin (A) and fibronectin (B) adsorbed on silane-PEG-COOH (SPC) coated and uncoated control (Ctrl) stainless steel surfaces. Much higher protein adsorption and concomitantly higher mean intensities were observed on uncoated steel surfaces than on silane-PEG-COOH coated surfaces regardless of the used protein. Used protein concentrations (C1 and C2) and exposure times (T1 and T2) are explained in the figure. Silane-PEG-COOH coated steel surface exposed to pure PBS (SPC +PBS), as a negative control, showed almost no fluorescence at all.

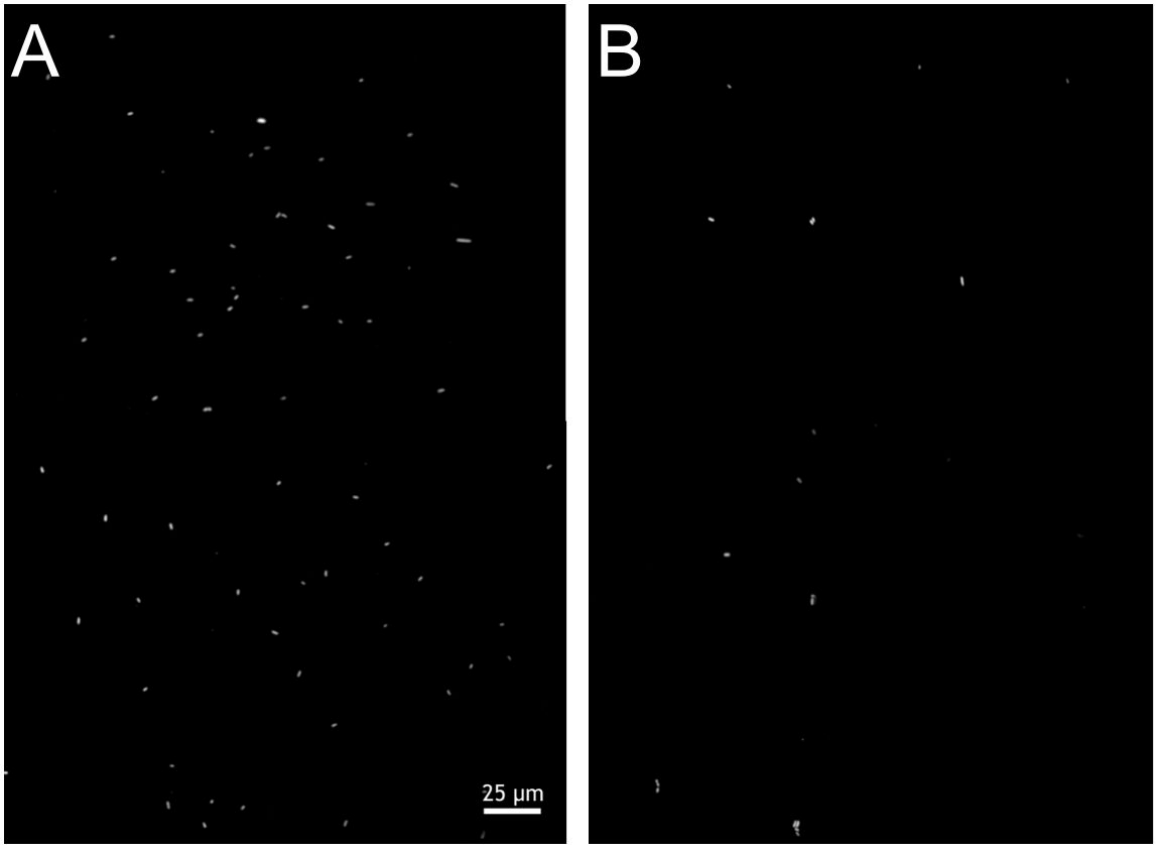

Figure 8. Silane-PEG derivative modifications noticeably reduce the attachment of bacteria to stainless steel surfaces. Fluorescence microscope images of *E.coli* bacteria attached to uncoated (A) and silane-PEG-COOH coated (B) steel surfaces are shown. Much less bacteria were observed on the silane-PEG coated surfaces than on the unmodified stainless steel.

5.2.2 *E. coli* adhesion test

Silanization of SS surfaces with both silane-PEG-COOH and silane-PEG-biotin has an apparent effect on reducing the attachment of bacteria on the surface (Figure 8). Also, both of the used silanization times (1 and 2 days) seem to have produced functional surfaces, since all silanized surfaces had less bacteria attached onto them than SS control samples (Figure 9). The medians of the number of attached bacteria (per a microscope image) were as follows: SS control 42 cells (n = 191, Interquartile range (IQR) = 25.0-90.0); 3 mg/ml silanization solution of silane-PEG-COOH with 2-day silanization 7.5 cells (n = 42, IQR = 3.4-28.3); 5 mg/ml silane-PEG-COOH 2d 11 cells

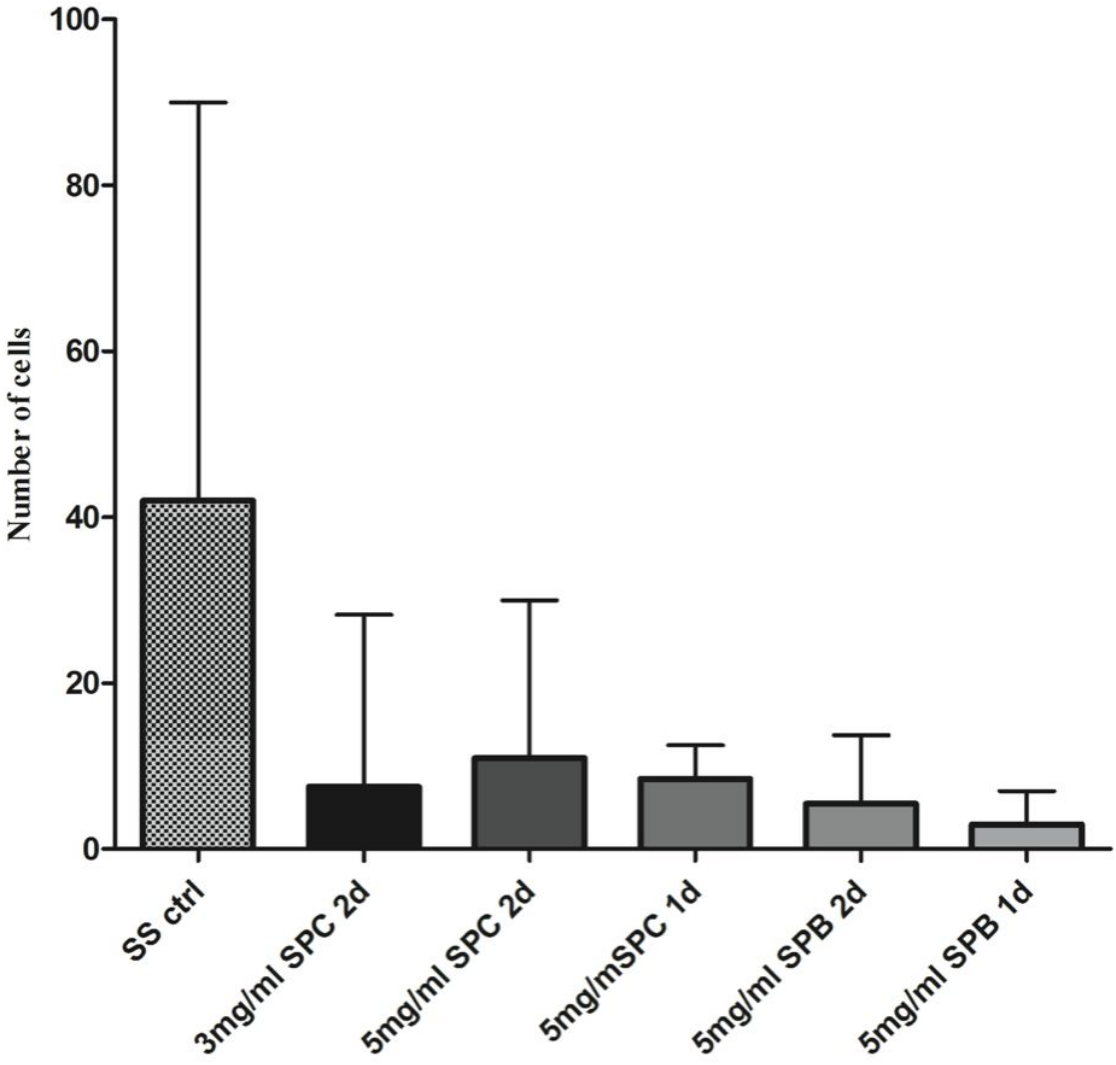

Figure 9. Number of attached E. coli cells observed on stainless steel surfaces with different kinds of silane-PEG derivative coatings after 1 h exposure test. Regardless of the coating type, silane-PEG-COOH (SPC) or silane-PEG-biotin (SPB), concentration of the silanization solution (3 or 5 mg/ml) or the silanization time (1 or 2 days) during surface preparation, the silane-PEG modifications seemed to significantly reduce the bacterial attachment when compared to unmodified stainless steel (SS ctrl). Median and interquartile range are depicted.

(n = 55, IQR = 5.0-30.0); 5 mg/ml silane-PEG-COOH 1d 8.5 cells (n = 20, IQR = 6.0-12.5); 5 mg/ml silane-PEG-biotin 2d 5.5 cells (n = 10, IQR = 2.8-13.8); and 5 mg/ml silane-PEG-biotin 1d 3 cells (n = 20, IQR = 2.0-7.0). Thus, the amount of bacteria on silanized surfaces reduced 75 % or more as compared to that observed in the SS controls. Accordingly, statistically significant difference was found between the SS control and all silanized samples (Kruskal-Wallis test with Dunn's post hoc test, $p<0.05$). However, no statistical differences were discovered among the silanized samples, and, thus, none of the silanization protocols can be said to have produced distinctively better coating in terms of preventing bacterial adherence when compared to each other. Furthermore, the results were rather consistent regardless of the used silane-PEG derivative which indicates that the end group of silane-PEGs (COOH or biotin) does not notably disrupt or otherwise affect the antifouling properties of the silane layer.

5.2.3 Avidin detection on silane-PEG-biotin surfaces

5.2.3.1 Spectrophotometric assay

Interaction and adherence of avidins with silane-PEG-biotin coated surfaces was studied by adding streptavidin-alkaline phosphatase (SA-AP) conjugates to the coated surfaces. After adding the substrate for SA-AP the amount of bound molecules could be assessed spectrophotometrically from the colorful reaction product of SA-AP and pnPP substrate (Figure 10). Compared to the controls, the absorbance and, thus, the amount of bound SA-AP was found to be highest with the actual silane-PEG-biotin + SA-AP samples. This suggests successful surface functionalization and specific binding of SA-AP to silane-PEG-biotins on the SS (average absorbance at the 60 min time point was 0.571), even though rather large deviations were observed between the samples. However, on average a continuous positive trend was apparent. In addition, the negative controls where functionalization was prevented by blocking the biotin binding site of SA-AP with free biotin, showed very little SA-AP adhesion and insufficient functionalization (absorbance maximum at 120 min time point was 0.075). Therefore, the interaction between SA-AP and surface-bound biotin can be considered efficient and vital with regard to the functionalization. Surprisingly though, the other negative control surfaces coated with silane-PEG-COOH showed moderate SA-AP binding (average absorbance at 60 min time point was 0.312), even though no biotins existed on the sample surfaces. Unfortunately, absorbances could not be measured at 120 min time point for all samples

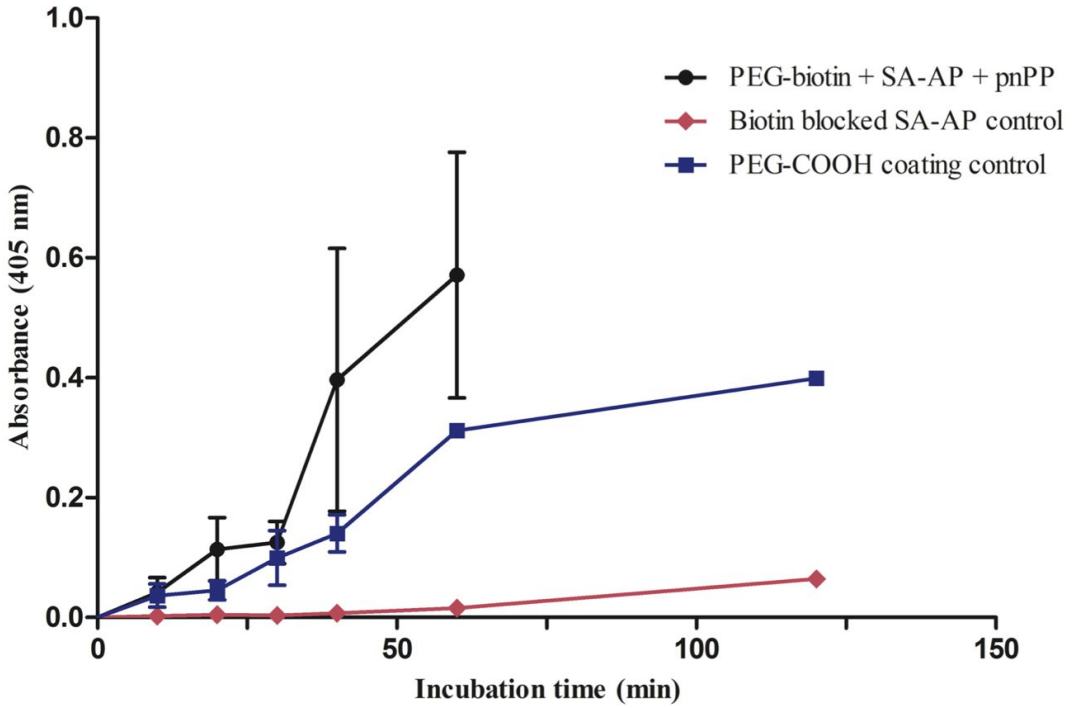

Figure 10. Spectrophotometric avidin detection assay. Streptavidin alkaline phosphatase conjugate (SA-AP) was linked to silane-PEG-biotin coated stainless steel surface. By adding the pnPP substrate of alkaline phosphatase, the amount of the surface-bound streptavidin was assessed based on the amount of spectrophotometrically detected reaction product. The black line depicts the actual samples, and noticeable binding of SA-AP was detected. The blue and red lines are negative controls. The blue line had silane-PEG-COOH coated stainless steel so that there were no biotins on the surface for the SA-AP to bind. Surprisingly, moderate binding was observed. The red line had the SA-AP blocked by biotin so that no further binding to silane-PEG-biotin coated surface could not occur. Consequently, only negligible binding was detected. Average absorbances and standard deviations are depicted where possible.

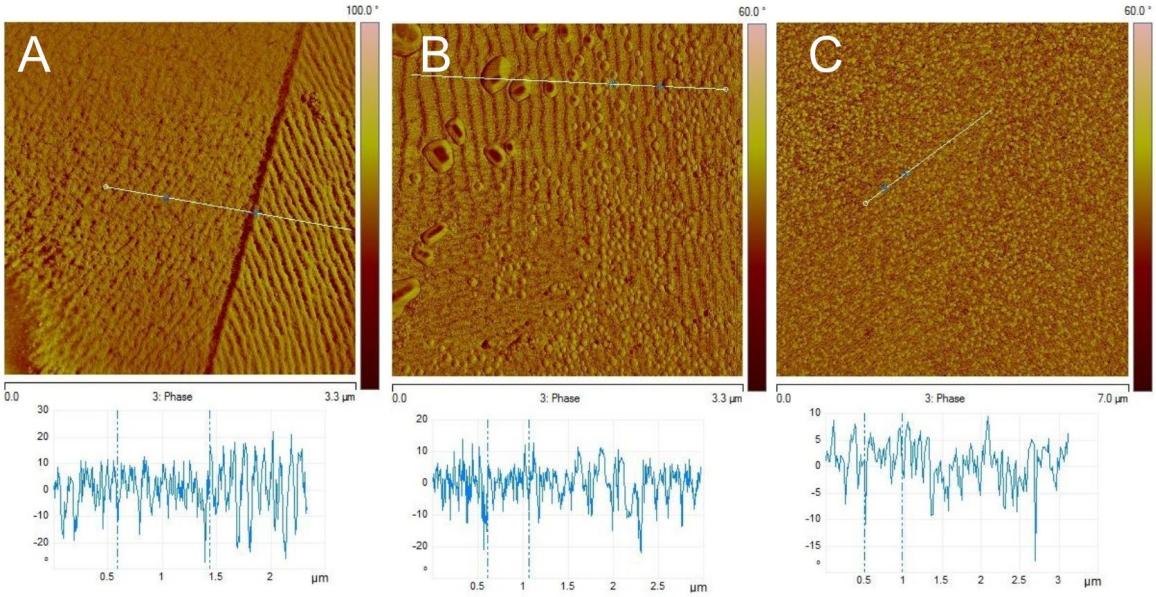

Figure 11. AFM images of avidins linked on silane-PEG-biotin (SPB) coated stainless steel surfaces. A. 3 x 3µm phase image of a reference SPB surface without avidins. B. 3 x 3 µm phase image of SPB surface with avidins. The smaller dots are expected to be avidins. The bigger dots with dark cores are most likely aggregates of water, salts or avidins. C. 7 x 7 µm phase image of a SPB surface with avidins. The avidins appear as bright dots on the image. Cross-section topographies of the surfaces are also shown. The z-axis scale is shown next to the images in nanometers.

and, hence, the trend of the curve over the 60 min time point could neither be reliably estimated nor reported for all of the cases.

5.2.3.2 Avidin detection with atomic force microscopy

Avidin functionalization of silane-PEG-biotin coated SS was also studied with AFM. As with the silane-PEG-COOH samples, the morphology of the silane-PEG-biotin coated SS samples did not noticeably diverge from the plain SS controls and the typical grooves and domains of SS were again clearly visible. Grooves were measured to be 5-10 nm high and according to the phase images the groove dips of silanized samples varied from -1° to -4°, which is in good agreement with the results obtained with silane-PEG-COOH coated surfaces. However, in the case of avidin functionalized silane-PEG-biotin samples, small 5-20 nm particles could be observed on the surface (Figure 11). Particles of the size of approximately 5 nm seemed to be rather homogenous and their size corresponds well to the known dimensions of avidins, which are cylindrical and about 5 nm long (Leppiniemi et al. 2011). The particles, i.e. presumably the avidins, are not, however, evenly distributed on the whole sample surface and, thus, the density and amount of the functionalization of the surface is not uniform. The larger particles on the surfaces were more heterogenous and oftentimes appeared to have darker core in the phase images, which suggests that they consisted of water, salts, avidin clusters or possibly combinations of them all.

6 Discussion

6.1 Surface characterization

Surfaces that are in frequent contact with biological substances should in many occasions be modified in order to improve their biocompatibility or to enhance their beneficial properties. One of the most used method, especially when fighting against biofouling, is to coat the surfaces with a layer consisting of PEG chains. PEGs are considered ideal due to their excellent chemical properties, such as inertness, good solubility in various solvents and non-toxicity as well as non-immunogenicity. In addition, PEG chains can also be readily modified and linked to other molecules (Harris 1992).

PEG chains can be attached to surfaces via various methods, and in this thesis an approach based on silanization was chosen. The protocol itself was extremely straightforward, and allowed the silanization to be basically conducted in one simple step after the initial electrochemical preparation of the stainless steel chips. Commercially available silane-PEG derivatives were used and the silanization was performed by immersing the SS samples in the silanization solution for a certain amounts of time. Thus, the chances for mistakes and human errors were minimized due to the small amount of steps required. Commercially obtained silane-PEG reagents also guaranteed the uniformity of the coating material, as no optimization for silane-PEG synthesis or cross linking conditions was needed. Overall the protocol was considered rather effortless and easily repeatable, and it was able to produce surfaces with desired and expected properties.

According to the XPS measurements the used protocol yielded rather uniform and extensively covered silane-PEG coated SS surfaces. In practice, the surfaces were completely covered and up to approximately 80 % of the coverage was homogenous in thickness and close to the expected dimensions, whereas the rest suffered from silane aggregation and other defects and, thus, could not be reliably measured. The chemical compositions of the coated surfaces were also determined to be alike, regardless of the concentrations of the applied silanization solution. However, alterations in the coating thickness were observed. Logically, however, silanization solutions with the lower, 3 mg/ml silane concentration resulted in thinner coatings, whereas the higher, 5 mg/ml solutions produced a thicker silane-PEG layer. Thus, the changes in silane concentration

did not significantly affect the chemistry of the silanes or the silanization process but rather merely changed the amount of silane-PEGs able to adhere on the surface. Nonetheless, the obtained surface coverage was not greatly affected by the concentration alterations. Overall, therefore, the applied silanization protocol appeared trustworthy and replicable in terms of the achieved surface quality.

In all measured conditions the thickness of the silane-PEG layer remained under 1 nm; approximately 0.6 nm on average. However, one silane-PEG 2000 molecule is expected to consist of approximately 50 ethylene oxide monomer segments and the mean monomer length is 2.78 Å (Carignano and Szleifer 2000; Oesterhelt et al. 1999). Hence, the theoretical maximum length of a completely extended silane-PEG 2000 molecule would be over 13 nm which clearly exceeds the measured silane layer thickness of less than 1 nm. This suggests that the silane-PEGs most likely are not very organized and standing in upright conformation next to each other but instead lie as a mesh close to the steel surface. However, this might a be consequence from the packing density of the PEG chains, since according to the XPS data the silane-PEGs are not attached very close to each other. Thus, the PEG chains have plenty of lateral space to spread out. In a denser packing situation, though, the PEG chains would have been forced to preferentially extend upwards from the surface and, hence, increase the thickness of the coating. Moreover, in the literature surface-grafted PEG layers are generally measured and reported to be thicker than the above presented results, which further suggests that optimization in terms of PEG surface density ought to be considered. For example, Wei et al. (2003) had achieved close to a six nanometers thick PEG (M = 5000) coating on poly(ethylenimine) (PEI) functionalized stainless steel, and Jo and Park (2000) reported to have prepared a two nanometers thick PEG (M = 5000) layer on glass substrate by silanization. However, it should be noted that both groups used PEG-5000 molecules, which are over 2.5-times longer than the PEG-2000 used in this study. When considering smaller PEGs, though, for example Zhang et al. (1998) have successfully immobilized PEG-SiCl (M = 600) derivatives onto silicon surfaces and reported coating thickness of approximately 0.5 nm. Hence, higher density and spatial organization seem to be rather critical for the thickness.

The low packing density of the silane-PEGs on the surface is also supported by the fact that no consistent network of siloxane bonds was detected with the XPS. For example, smaller APS molecules are known to extensively bond with the surface as well

as with each other through their silane groups when in a monolayer structures on stainless steel, which has also been confirmed by XPS measurements (Jussila et al. 2010). However, similar bonding behavior and resultant Si atom layer in XPS depth profiling were not detected here with the silane-PEGs. This implies that in the studied silane-PEG coatings the silane end-groups of the coating are not located close enough to each other, or possibly even to the surface, in large enough of amounts to form the siloxane network and, consequently, to be able to be detected with the XPS. Thus, the covalent bonding and the organization of the silane end-groups of the silane-PEGs on SS surfaces could not be reliably confirmed. Therefore, it may be possible that instead of covalent bonding the silane-PEGs are attached to the surfaces through physisorption. This however, is completely opposite to the initial expectations and it is also probable that PEGs, that would have been attached to the surfaces only through physisorption, would have been washed off from to the surfaces during the experiments. Hence, at least some covalent bonding is likely to have occurred, even though the dense siloxane network could not be detected. Additionally, the silane-PEG chains were, nonetheless, able to spread out so effectively that the above mentioned extensive surface coverage could be established.

Since the silane-PEGs are not standing strictly next to each other on the SS surfaces as hypothesized, the additional heating step in the silanization protocol appears to be somewhat trivial and unnecessary. As in the case with the smaller APS molecules, the heating step is utilized to facilitate the covalent coupling between the silane groups of the adsorbed molecules and enhance their binding with the steel surface as well as with each other, by converting the initial hydrogen bonds into covalent bonds. This should make the resulting silane coating more rigid and durable (Jussila et al. 2010). Unfortunately though, the random and scarce positioning of the silane groups of the silane-PEGs on the stainless steel most likely renders the heating step inefficient.

According to the contact angle measurements the heating, nonetheless, seems to have an effect on the hydration state of the silane-PEG coating, and makes the coated surfaces a little more hydrophobic (Figure 5). Even though the difference was not statistically significant between all heated samples and their respective non-heated controls, and the changes in the measured contact angles are in the range of approximately 3-5 degrees, overall the trend appears to exist and to be of similar nature regardless of the used silane-PEG derivative (silane-PEG-COOH or silane-PEG-biotin).

However, the observed differences may be mainly a consequence from the alterations in the total water content inside the silane-PEG layer instead of actual changes in the composition of the silane-PEG coatings. The heating step might have vaporized some intrinsic water from the silane-PEG layers which consequently would affect the abilities of the PEG chains, since the mutual interactions between PEG chains and the surrounding water are considered to be of utmost importance for the proper functionality of all coatings utilizing PEG chains (Besseling 1997; Wang et al. 1997). Most importantly, it has been proposed that the antifouling properties of PEGylated surfaces depend on the ability of the PEG molecules to arrange nearby water molecules in a favorable way to prevent undesired adsorption, as for example Andrade and de Gennes (Jeon et al. 1991), Besseling (1997) and Grunze (Wang et al. 1997) have suggested. Therefore, the exclusion of water from the coated surfaces by heating might intercept this critical cooperation.

If the observed changes in the contact angle measurements due to the heating are actually a result of the vaporization and exclusion of intrinsic water from the heated samples instead of the changes in the physicochemical state or properties of the silane-PEG molecules themselves, it could be possible that these alterations could be reversed and fixed by re-hydrating the samples after the heating by, for instance, immersing them in water for some period of time to allow them to regain and organize their lost intrinsic water content. Then by measuring the contact angles of samples before and after the rehydration should give some implications whether or not the observed difference is merely caused by the drying of the samples or does it in fact reflect true changes in the silane-PEGs themselves. However, this rehydration experiment was not carried out under this project and, hence, this speculation could not be concluded. In the future, though, it would be valuable to find out how and what kinds of changes the heating steps really brings about in the silane-PEG coatings and the notion should be further investigated.

In general, the silane-PEG coating reduced the hydrophobicity of the stainless steel surfaces in all cases (Figure 5). The measured contact angles were approximately 10 degrees lower for the coated and non-heated samples than for the uncoated stainless steel controls. The differences were statistically significant. The differences between control and the heated silanized samples were also of similar nature but, however, not statistically significant. Additionally, no statistically significant differences were found

between the different silane-PEG derivative coatings, which had been prepared according to the same protocol, i.e. with or without the additional heating step. In all cases, including the uncoated SS controls, though, the measured contact angles remained clearly under 60º. According to some studies the contact angle values close to the 60º limit has been determined as a sort of a borderline between protein adsorptive and non-adsorptive materials, since the transition over the 60-65º region has been shown to yield in a distinct changes in protein adsorption behavior (Berg et al. 1994; Xu and Siedlecki 2007). Additionally, minor changes outside this 60º to 65º degree region has been suggested to be negligible or at least less important in terms of protein adsorptivity. Hence, considerable benefits regarding the surface hydrophobicity cannot be said to have been achieved. Even though, the surfaces became more hydrophilic due to the silane-PEG coating, the actual changes remained rather small. Additionally, the contact angle values of the clean stainless steel surfaces were already found to reside in the more favorable, i.e. the poorly protein adsorbing, side of the above mentioned 60º limit. Thus, the obtained changes in the surface hydrophilicity, even though positive and in desired direction, at least according to the theory presented above, are not very important or driving factors regarding the resulting antifouling properties of the modified surfaces, but rather supportive and pleasant byproducts of the coating process. In conclusion, the observed improved protein and bacterial adhesion resistance of the silane-PEG coated stainless steel surfaces, therefore, presumably stems from other features of the coating than its increased surface hydrophilicity.

AFM imaging of the prepared surfaces revealed some surprising results as the silane-PEG coating could not be directly seen on the samples as expected (Figure 3). Even the phase images, that especially highlight changes in e.g. surface composition and viscoelasticity, were unable to clearly visualize the attached silane-PEG layer. Apart from some clusters, consisting of silane-PEGs, salts or liquid, and other nanosized particles, that were most likely dust or other impurities from the environment, the silane-PEG coated and uncoated control surfaces appeared nearly identical and the typical domains and surface characteristics of stainless steel could be detected on all samples regardless of the silane-PEG-coating. Hence, no direct supportive data for the XPS measurements about the uniformity, coverage and overall quality of the silane-PEG coating could be gathered. However, the transparency of the coating in the AFM images suggests that the layer is indeed very thin as was also claimed by the XPS analysis.

Since in an optimal situation the whole steel sample surface would be covered by a dense monolayer of silane-PEGs, the combined results of the XPS and AFM measurements that indicated the existence of an extremely thin but, nonetheless, extensive silane-PEG coating, are very encouraging.

Additionally, AFM images revealed that in silanized samples some substance was found to reside in the grooves of the steel surface and also made the groove dips less steep compared to the clean control samples. Even though the substance could not be accurately identified, it most likely consisted of the silane-PEG molecules that were gathered into the grooves. Hence, the images suggested that at least some silane-PEGs were able to attach to the surfaces, even though an uniform PEG layer could not be seen. Together with the XPS coverage analysis though, the results rather successfully validate the existence of the quite complete silane-PEG coating. Furthermore, this accumulation of the silane-PEGs into the grooves does not seem to be very significant, since in the AFM images no obvious deviations in the depth profiles between the coated and uncoated samples were found. Moreover, had the grooves had significant impact on the surface depth profile and the silane-PEG accumulation, it would have most likely been detected in the XPS measurements as the grooves are found allover the studied steel surfaces. However, noticeable silane-PEG aggregation was found in only about 15 % of the surface area. Therefore, minor aggregation of the silane-PEGs may exist, but only in such a small scale that it does not alter the overall surface topography, and the thickness of the silane-PEG layer stays rather constant despite the surface topography.

All in all, the used protocol was able establish thin but still rather complete and uniform silane-PEG coating onto stainless steel chips. The organization and binding pattern of the silane-PEGs could not be determined, though, but most likely they reside as a mesh network on the surface and relied considerably on non-covalent adsorption instead of covalent siloxane binding. Additionally, the coating layer followed the surface topography rather meticulously and did not significantly alter it, despite some aggregation in the surface grooves. The coating also made the surface more hydrophilic, even though the steel surfaces were already quite hydrophilic themselves before the silanization procedure.

6.2 Antifouling properties and selective avidin functionalization

Grafted PEG chains are known to prevent adsorption of e.g. proteins and bacteria on various surfaces, even though the actual mechanism is not completely known (Besseling 1997; Jeon et al. 1991; Szleizer 1997; Wang et al. 1997). According to the expectations the coated surfaces in this study also were able to substantially resist and decrease the biofouling of avidin and fibronectin proteins as well as *E. coli* bacteria. However, complete prevention of neither protein nor bacterial adhesion was achieved in any of the cases.

Antifouling surfaces consisting of PEG chains can be further modified to allow selective binding of certain molecules on the surface. In this case, silane-PEG-biotin coating was prepared, which was then further functionalized with avidins. The avidin functionalization protocol, similar to the original silanization protocol, was kept as simple and straightforward as possible. Thus, in this case the main focus was not on achieving the optimal functionalization rate and effectivity but instead simply on testing if the additional selective functionalization was possible. The results were overall positive, but undoubtedly there is still plenty of room for optimization and fine-tuning in the protocol.

In protein adhesion tests coated and uncoated steel surfaces were exposed to solutions of fluorescently labeled avidin and fibronectin for certain times, and the amount of adsorbed protein was then estimated by the mean fluorescence intensities of the microscope images taken from the samples. According to the results a clear, statistically significant reduction in the amount of adsorbed protein were found when comparing the silane-PEG coated samples to the plain stainless steel controls regardless of protein type (avidin or fibronectin), protein concentration (3 μg/ml or 30 μg/ml) and exposure time (1 h or 3 h). Thus, in all circumstances the silane-PEG coating remarkably improved the antifouling properties of the steel surface. Complete prevention of protein attachment was not achieved, though. Additionally, longer exposure times and higher protein solution concentrations seemed to positively correlate with the amount of the adsorbed protein.

Interestingly, the adsorption behavior of avidin and fibronectin were discovered to be very much alike and, additionally, the avidin even seemed to attach to the surfaces a bit more eagerly and in higher amounts than fibronectin (Figures 6 and 7). This could not be statistically confirmed, though. Moreover, avidin as a smaller and

more rigid protein, had not been expected to adhere to the surface as tightly as the naturally stickier and more adhesive fibronectin. However, the results might have been slightly biased due to the different fluorescent labeling ratios of the used proteins. The labeling ratio for avidin was 29.38 μmol of dye per 1 g of protein whereas for fibronectin the ratio was only 18.41, which might have benefitted avidin over fibronectin. Another aspect that may have affected the comparison was the tendency of fibronectin to aggregate and form fibrils on the surface, whereas avidins spread out rather evenly (Pellenc et al. 2006). As the mean intensity values of the images were used as a measure of the amount of adsorbed protein, the extensive spreading of avidins might have favored them over the local aggregates of fibronectin and, hence, possibly skewed the results (Figure 6).

Overall the protein adhesion test results were very encouraging as they showed that the prepared silane-PEG coatings actually were able to significantly reduce the adsorption of both of the proteins, avidin and fibronectin, on the steel surface. The magnitude of the reduction, in addition, was rather similar with both proteins, which suggests that despite the differences in the physicochemical natures of avidin and fibronectin, the coating managed to equally well regulate their adsorption. The amount of adhered proteins, hence, appeared to be mostly time and concentration dependent, whereas the specific protein characteristics seemed to have much lower impact than initially expected.

Similar observations have also been made by, for example, Yang et al. (2014) and Harder et al. (1998). Yang et al. have covered stainless steel surfaces with poly(ethylene oxide)-poly(propylene oxide)-poly(ethylene oxide) (PEO–PPO–PEO) triblock copolymer, and they found out that PEO-PPO-PEO modified surfaces were able to significantly reduce the adsorption of bovine serum albumin (BSA). However, without initial conditioning, a surface hydrophobization step, comparable in significance to the electrochemical surface passivation used in this study, they reported that the PEO-PPO-PEO merely adsorbed on the steel surface in different conformation and were not able to prevent protein adsorption. Moreover, Harder et al. (1998) have been able to create fibrinogen resistant surfaces on gold surfaces by using oligo(ethylene glycol)-terminated self-assembled monolayers (SAM). In addition, they discovered that similar SAMs on silver substrate failed to prevent fibrinogen adsorption due to differences in conformation and packing densities of the SAMs. Thus, PEGs and

PEG-like polymers are able to repel proteins as long as proper conformation and organization is guaranteed. Our results of avidin and fibronectin exposure tests on silane-PEGylated SS steel surfaces agree well with this antifouling trend of the PEGylated surfaces, and give no reason to believe that the modified steel surfaces as prepared here would be an exception. In accordance with Yang et al. (2014), this was further confirmed by also studying bacterial adhesion on the PEGylated surfaces, and as with the previously published studies, our results similarly showed a significant reduction in the amount of adhered bacteria on modified steel surfaces. Thus, we have been able to achieve a rather solid foundation for developing a completely antifouling steel surface and a promising starting point to extend the surface functionalization even further.

As mentioned above the silane-PEG coated steel surfaces were able to considerably resist bacterial adhesion onto them under the used experimental conditions. The *E. coli* bacteria were allowed to reside on the steel chips for 1 h after which they were fixed and fluorescently stained to allow microscope imaging and quantification (Figure 8). Complete prevention of bacterial adhesion was not achieved, though. The silane-PEG coating was able to reduce the amount of adhered bacteria approximately 75-95 % which is a significant improvement (Figure 9). However, the variation in the number of attached cells was rather considerable between the samples, also including the uncoated controls. Nonetheless, the difference existed and could be statistically confirmed.

The attachment of bacteria to silane-PEG coated steel surfaces was also investigated with SEM. The samples were prepared as in adhesion test and then sent to the University of Jyväskylä for SEM imaging. The goal was to inspect the quality of the coating as well as to see if it affected the attachment of the bacteria; i.e. did the bacteria prefer or specifically bind to sites with flawed coating, silane-PEG aggregates or other surface defects, for instance. Unfortunately though, no hypothesized differences in the adhesion characteristics between the coated and uncoated surfaces could be detected (Figure 4). However, the used sample size was very small and, therefore, it would be reasonable to replicate the experiment before any actual conclusions are made. A case in point Gon et al. (2012) have reported that cationic polymer patches, that are incorporated into a PEG layer to mimic flaws in the coating, attract bacteria and as a result facilitate their attachment. Even though they used a different bacterial strain

(*Staphylococcus aureus*) and assessment methods, their observations are, nonetheless, opposite to the ones obtained here with SEM.

Another very interesting report is from Wei et al. (2003) who have reported that stainless steel (AISI 316) modified with PEGs (molecular weight 5000) is able to resist protein adsorption but not bacterial attachment. They used a two-step PEGylation method with poly(ethylenimide) (PEI) and methoxy-terminated aldehyde-PEGs (M-PEG-CHO). For adhesion test they used β-lactoglobulin protein solution and both *Pseudomonas* sp. and *Listeria monocytogenes* bacterial strains. Their result showed that the PEGylated surface at the highest graft density, that they were able to achieve, was capable of preventing protein adsorption, which is in good accordance with our protein adsorption tests. With the bacteria, however, they found no differences between the tested surfaces regardless of PEGylation. It should be noted, though, that the exposure time, which was used by Wei et al. (2003), differs from the one used in this study, which might explain the variations in the results. They used 24 h immersion whereas the bacterial adhesion test used here had only 1 hour exposure. Nevertheless, they reported full bacterial saturation levels to have been achieved already within first couple of hours in most cases, which somewhat contradicts with our observations. Obviously Wei et al. used different kinds of bacterial strains and their exposure test conditions were different from ours, as they utilized stirring to create a dynamic environment whereas a platform shaker and gentle agitation was used here, but still the results are rather surprising. Thus, our experiments with longer incubation times ought to be tested to allow more direct comparison and to find out if the observed differences actually are valid. Naturally different bacterial strains and proteins as well as the size of the used PEG may have an impact, but the effect of different exposure times should, however, be further investigated.

As the silane-PEG modified surfaces successfully managed to express the desired antifouling characteristics, further functionalization through specific intermolecular binding was also tested. SS surfaces coated with silane-PEG-biotin were exposed to avidin solution and as a results avidins were expected to be able to attach to the biotins on the surface. Consequently, another layer of functionalization ought to have been added onto the antifouling surface. The rate of avidin functionalization was evaluated with AFM and a spectrophotometric assay.

AFM images of the avidin functionalized surfaces showed that indeed some 5-nm particles were attached to the surfaces (Figure 11). In addition, most of the particles were rather homogenous and in the known size range of avidins and, hence, suggested that the functionalization was successful. However, a subset of the observed particles were much larger than avidins and they were thought to be aggregates of liquid, salts or avidins. Nonetheless, according to the AFM images the avidins seemed to be able to attach to the surface-bound silane-PEG-biotins. However, the achieved quality of the functionalization was not uniform over the whole surface, since the distribution of the particles on the surfaces was quite heterogenous and had distinctive local deviations. This suggests that the biotins on the surface may not have been properly available for the avidins to bind. Since the PEG chains were believed to lie as a mesh close to the surface, the biotins could have possibly been buried under the PEGs which consequently would have prevented the interaction with avidins. However, this hypothesis could not be confirmed and the problem might as well lie in the unoptimized functionalization protocol. Nonetheless, if selective binding is utilized in the surface functionalization in the future, the proper presentation of the surface-bound functionalization groups is of utmost importance and, thus, should be appropriately and more thoroughly considered.

The spectrophotometric assay of the avidin functionalization also suggested that the functionalization had succeeded and provided supportive evidence for the AFM images; the observed intensity was obviously higher in the functionalized samples than in negative controls, which agrees with the data acquired from the AFM images (Figure 10). However, one of the negative control samples with silane-PEG-COOH surface surprisingly was able to bind some SA-AP and, thus, achieve some level of functionalization, even though there should not have been any molecules on the surfaces where the avidins could have attached. The extent of functionalization stayed lower than on the actual samples, though, but he reason for this unspecific binding is unknown. The possible electrostatic attraction is not considered plausible, since both the silane-PEG-COOH surface and the streptavidin-alkaline phosphatase conjugate are expected to be negatively charged at basic pH environment and, hence, to repel each other, as the pI of streptavidin is between 5 and 6 (Diamandis and Christopoulos 1991) and the pI of alkaline phosphatase is 4.5 (Garen and Levinthal 1960). However, by performing another control experiment with some other silane-PEG derivative it could be

confirmed, whether or not the binding was actually caused by the carboxylic acid groups of the silane-PEG coating. Despite the surprising results with COOH-terminated PEGs, though, a distinctive and desired difference between the actual samples and the controls was observed.

6.3 Future perspectives

Generally speaking all of the above presented results have been encouraging and positive as well as adequately well in line with the initial expectations. Remarkably they have also been achieved with rather simple and user-friendly methods which provides a solid starting point and a useful frame for future experiments and further optimization. One especially important approach in the future experiments would be the use of different kinds of silane-PEGs to see if the results could be further improved by merely adjusting the type of the coating material. For example, branched-chain PEGs have been shown to be able to form better antifouling coatings than linear single-chain PEGs, such as the ones used in this study (Szleifer 1997). The branched-chain PEGs are able to spread out more effectively than the single-chain PEGs and as a result they also create a much higher local PEG density on the surfaces. This consequently causes a stronger steric barrier to resist e.g. protein adsorption. Alternatively, multiple functional groups, that bind the PEGs to surfaces, e.g. silane groups, could be added to the PEG chains. For instance, bifunctional single-chain PEGs with two surface-adhering groups have been shown to bind surfaces more efficiently than analogous mono-adhering PEGs of similar size. In addition, the PEGs utilizing multiple adhesion groups are more effective at preventing non-specific adsorption due to their more strictly determined spatial orientation and heavier localization closer to the surface (Szleifer 1997).

One interesting method to adjust surface properties would also be the use of mixtures of different kinds of PEGs or even PEGs and some other polymers. For example, Carignano and Szleifer (2000) have claimed that optimal coatings to obtain large reduction of protein adsorption and availability of functional groups for binding are achieved by utilizing mixtures of flexible and stiff, rod-like molecules. The flexible chains are considered to be superior in forming dense antifouling layer close to surfaces, whereas the stiffer polymers extend far into the surroundings and both broaden the steric barrier and provide excellent targets for selective additional binding and functionalization. Hence, especially from the point of view of surface functionalization

it might beneficial to use stiff rods to present the functional groups out of the otherwise antifouling surface.

Finally, to obtain a fully comprehensive view of the potential of the modified surfaces, the methods presented in this study should still be carefully optimized and fine-tuned, as has already been mentioned, but also new tests and experiments ought to be designed and added. For instance, eukaryotic cells have been omitted from this thesis and the effects of silane-PEG coating to those cells has not been studied, even though the interaction between surfaces and especially mammalian cells is vital for numerous applications, for instance, orthopedic implants. Furthermore, specific surface functionalization provides intriguing possibilities among others to cell culture technology, where for example growth inducers and hormones could be attached to surfaces to guide stem cell proliferation and differentiation.

From a practical point of view, the experiments should also be modified to include longer time-scale tests than presented here. Firstly, the coatings and the whole modified surfaces ought to be proven to endure and survive long-term stress and usage before they can actually be considered to be utilized in practical applications. Secondly, as Miller et al. (2012) have demonstrated, short term batch adhesion tests with model proteins or bacteria under static conditions may not correlate accurately with the long-term antifouling potential. Thus, longer time-scales as well as more dynamic experimental conditions are needed to reliably assess the total capability and usefulness of the modified surfaces, even though the results so far appear promising and encouraging.

7 Conclusions

The results presented here show that the silanization with silane-PEG derivatives is indeed a noteworthy method for modifying the biocompatibility of stainless steel surfaces. The outcomes generally expressed a positive trend and were well in line with the initial expectations, even though the experimental setup and the silanization protocol were simple and rather unpolished as full optimization could not be conducted within the time frame of this thesis. Nonetheless, the surface characterization methods revealed that the silanization protocol could be successfully used to modify SS surfaces, and the hydrophilicity and chemical composition of the surfaces were altered due to the silanization. The produced coating was also found to be thin, yet still homogenous and extensive. Sadly, the attachment of the silanes to the surface via covalent bonding could not be confirmed. Nevertheless, the silane-PEG layer was able to remarkably affect the functionality of the surfaces and reduce the attachment of both proteins and bacteria. Complete prevention of adhesion was not achieved in neither of the cases, though. Yet with some modifications and further optimization the results can still be expected to be noticeably improved. In addition, specific functionalization of the modified steel surfaces was proved possible by using silane-PEG-biotin coatings and avidins. Even though lots of work is still needed, the concept of functionalization via selective binding, however, appeared already rather effective. This provides interesting possibilities in the future as the protocol could in theory be utilized to add nearly any molecules on the surfaces as long as suitable derivatives of the surface coating reagents are available.

All in all, the results have been encouraging and important steps have been taken towards possible practical applications e.g. in medical or biotechnological fields. However, the methods presented here are still incomplete and further optimization is undoubtedly required. Especially, the use of different kinds of PEGs and mixtures of polymers ought to be considered and their behavior studied, as they would allow another level of control into the fine-tuning and adjustment of the surface properties. Also experiments covering longer timescales and more dynamic conditions should provide essential information and help to close the gap between pure experimental setup and real-life situations.

References

Al-Ahmad M, Wiedmann-Al-Ahmad A, Fackler M, Follo E, Hellwig M, Bächle C, Hannig J-S, Han M & Wolkewitz R. In vivo study of the initial bacterial adhesion on different implant materials. Archives of Oral Biology. 2013;58(9):1139-47A.

Anderl JN, Zahller J, Roe F & Stewart PS. Role of nutrient limitation and stationary-phase existence in Klebsiella pneumoniae biofilm resistance to ampicillin and ciprofloxacin. Antimicrob Agents Chemother. 2003;47:1251–6.

Andrade JD, Hlady V & Wei AP. Adsorption of complex proteins at interfaces. Pure Appl Chem. 1992; 64(11):1777-81.

Becker J, Kirsch A, Schwarz F, Chatzinikolaidou M, Rothamel D, Lekovic V, Laub M & Jennissen HP. Bone apposition to titanium implants biocoated with recombinant human bone morphogenetic protein-2 (rhBMP-2). A pilot study in dogs. Clin Oral Investig. 2006;10(3):217-24.

Benhabbour SR, Sheardown H & Adronov A. Cell adhesion and proliferation on hydrophilic dendritically modified surfaces. Biomaterials. 2008;29(31):4177-86.

Berg JM, Eriksson LGT, Claesson PM & Borve KGN. 3-Component Langmuir–Blodgett-films with a controllable degree of polarity. Langmuir 1994;10(4):1225–34.

Besseling NAM. Theory of Hydration Forces between Surfaces. Langmuir. 1997;13(7): 2113–22.

Cai KY, Bossert J & Jandt KD. Does the nanometre scale topography of titanium influence protein adsorption and cell proliferation? Colloids Surf B Biointerfaces. 2006;49(2):136–44.

Carignano MA & Szleifer I. Prevention of protein adsorption by flexible and rigid chain molecules. Colloids Surf B Biointerfaces. 2000;18(3-4):169-82.

Daly SM, Przybycien TM & Tilton RD. Coverage-Dependent Orientation of Lysozyme Adsorbed on Silica. Langmuir. 2003;19(9):3848–57.

Demanèche S, Chapel JP, Monrozier LJ & Quiquampoix H. Dissimilar pH-dependent adsorption features of bovine serum albumin and α-chymotrypsin on mica probed by AFM. Colloids Surf B Biointerfaces. 2009;70(2):226-31.

Diamandis EP & Christopoulos TK. The Biotin-(Strept)Avidin System: Principlesand Applicationsin Biotechnology. 1991; 37(5):625-636.

Dibdin GH, Assinder SJ, Nichols WW & Lambert PA. Mathematical model of β-lactam penetration into a biofilm of Pseudomonas aeruginosa while undergoing simultaneous inactivation by released β-lactamases. J Antimicrob Chemother. 1996;38:757–69.

Espeland EM & Wetzel RG. Complexation, stabilization and UV photolysis of extracellular and surface-bound glucosidase and alkaline phosphatase: implications for biofilm microbiota. Microb Ecol. 2001;42:572–85.

Flemming HC & Schaule G. Biofouling on membranes - A microbiological approach. Desalination. 1988;70(1-3):95-119.

Gallo J, Kolár M, Novotný R, Riháková P & Tichá V. Pathogenesis of prosthesis-related infection. Biomed Pap Med Fac Univ Palacky Olomouc Czech Repub. 2003;147(1): 27-35.

Garen A & Levinthal C. A Fine-Structure Genetic and Chemical Study of the Enzyme Alkaline Phosphatase of *E. coli.* I. Purification and Characterization of Alkaline Phosphatase , Biochim Biophys Acta. 1960;38:470-83.

Gon S, Kumar KN, Nüsslein K & Santore MM. How Bacteria Adhere to Brushy PEG Surfaces: Clinging to Flaws and Compressing the Brush. Macromolecules. 2012;45(20): 8373-81.

González-García C, Sousa SR, Moratal D, Rico P & Salmeron-Sanchez M. Effect of nanoscale topography on fibronectin adsorption, focal adhesion size and matrix organisation. Colloids Surf B Biointerfaces. 2010;77(2):181–90.

Guégan C, Garderes J, Le Pennec G, Gaillard F, Fay F, Linossier I, Herry JM, Fontaine MN & Réhel KV. Alteration of bacterial adhesion induced by the substrate stiffness. Colloids Surf B Biointerfaces. 2014;114:193-200C.

Hall-Stoodley L, Costerton JW & Stoodley P. Bacterial biofilms: from the natural environment to infectious diseases. Nat Rev Microbiol. 2004;2(2):95-108.

Hannula M. Silanointiparametrien vaikutus sähkökemiallisesti apssivoidun austeniittisen teräksen pinnalle rakentuvan biofunktionaalisen seossilaaniohutkalvon koostumukseen. Technical University of Tampere, Master of Science Thesis. 2013.

Harder P, Grunze M, Dahint R, Whitesides GM & Laibinis PE. Molecular conformation in oligo(ethylene glycol)-terminated self-assembled monolayers on gold and silver surfaces determines their ability to resist protein adsorption. J Phys Chem B. 1998;102(2):426–36.

Harris JM. Poly (ethylene glycol) chemistry: biotechnical and biomedical applications. Springer. 1992:1-12. ISBN 0-306-44078-4.

He ZY, Chu BY, Wei XW, Li J, Edwards CK 3rd, Song XR, He G, Xie YM, Wei YQ & Qian ZY. Recent development of poly(ethylene glycol)-cholesterol conjugates as drug delivery systems. Int J Pharm. 2014;469(1):168-78.

Hirsh SL, McKenzie DR, Nosworthy NJ, Denman JA, Sezerman OU & Bilek MM. The Vroman effect: Competitive protein exchange with dynamic multilayer protein aggregates. Colloids Surf B Biointerfaces. 2013;103:395-404.

Jeon SI, Lee JH, Andrade JD & De Gennes PG. Protein—surface interactions in the presence of polyethylene oxide: I. Simplified theory. J Colloid Interface Sci. 1991; 142(1):149-58.

Jo S & Park K. Surface modification using silanated poly(ethylene glycol)s. Biomaterials. 2000;21(6):605-16.

Jones KL & O'Melia CR. Protein and humic acid adsorption onto hydrophilic membrane surfaces: effects of pH and ionic strength. J Membr Sci. 2000;165(1):31-46.

Jussila P, Ali-Löytty H, Lahtonen K, Hirsimäki M, & Valden, M. Effect of surface hydroxyl concentration on the bonding and morphology of aminopropylsilane thin films on austenitic stainless steel. Surf Interface Anal. 2010;42(3):157–64. DOI: 10.1002/sia. 3200.

Kane RS, Deschatelets P & Whitesides GM. Kosmotropes Form the Basis of Protein-Resistant Surfaces. Langmuir. 2003;19(6):2388–91.

Kasemo B. Biological surface science. Surf Sci. 2002;500(1–3): 656-77.

Kingshott P & Griesser HJ. Surfaces that resist bioadhesion. Curr Opin Solid State Mater Sci. 1999;4(4):403-12.

Klausen M, Heydorn A, Ragas P, Lambertsen L, Aaes-Jørgensen A, Molin S & Tolker-Nielsen T. Biofilm formation by Pseudomonas aeruginosa wild type, flagella and type IV pili mutants. Mol Microbiol. 2003;48(6):1511-24.

Koutsoukos PG, Norde W & Lyklema J. Protein adsorption on hematite ([α]-Fe2O3) surfaces. J Colloid Interface Sci. 1983;95:385–97.

Kunz W, Henle J & Ninham BW. 'Zur Lehre von der Wirkung der Salze' (about the science of the effect of salts): Franz Hofmeister's historical papers. Curr Opin Colloid Interface Sci. 2004;9(1-2):19-37.

Lahtonen K, Lampimäki M, Jussila P, Hirsimäki M, & Valden M. Instrumentation and analytical methods of an X-ray photoelectron spectroscopy–scanning tunneling microscopy surface analysis system for studying nanostructured materials. Rev Sci Instruments. 2006;77(8):083901-1–083901-9. DOI: 10.1063/1.2221539.

Le Magrex-Debar E, Lemoine J, Gelle MP, Jacquelin LF & Choisy C. Evaluation of biohazards in dehydrated biofilms on food stuff packaging. Int J Food Microbiol. 2000;55(1-3):239–43.

Leid JG, Shirtliff ME, Costerton JW & Stoodley P. Human leukocytes adhere, penetrate, and respond to Staphylococcus aureus biofilms. Infect Immun. 2002;70:6339–45.

Leppiniemi J, Määttä JA, Hammaren H, Soikkeli M, Laitaoja M, Jänis J, Kulomaa MS, & Hytönen VP.Bifunctional avidin with covalently modifiable ligand binding site. PLoS One. 2011;6(1):e16576. doi: 10.1371/journal.pone.0016576.

Lord MS, Foss M & Besenbacher F. Influence of nanoscale surface topography on protein adsorption and cellular response. Nano Today. 2010;5(1):66-78.

Luk YY, Kato M & Mrksich M. Self-Assembled monolayers of alkanethiolates presenting mannitol groups are inert to protein adsorption and cell attachment. Langmuir. 2000;16(24):9604-08.

Mah TF & O'Toole GA. Mechanisms of biofilm resistance to antimicrobial agents. Trends Microbiol. 2001;9(1):34-9.

Maller RR. Passivation of stainless steel. Trends Food Sci Technol. 2007;18:S112-S115.

Malmsten M, Emoto K & van Alstine JM. Effect of Chain Density on Inhibition of Protein Adsorption by Poly(ethylene glycol) Based Coatings. J Colloid Interface Sci. 1998;202(2):507-17.

McColl J, Yakubov GE, Ramsden JJ. Complex desorption of mucin from silica. Langmuir. 2007;23(13):7096-100.

Michu E, Cervinkova D, Babak V, Kyrova K & Jaglic Z. Biofilm formation on stainless steel by Staphylococcus epidermidis in milk and influence of glucose and sodium chloride on the development of ica-mediated biofilms. Int Dairy J. 2011;21:179-84.

Miller DJ, Araújo PA, Correia PB, Ramsey MM, Kruithof JC, van Loosdrecht MC, Freeman BD, Paul DR, Whiteley M & Vrouwenvelder JS. Short-term adhesion and long-term biofouling testing of polydopamine and poly(ethylene glycol) surface modifications of membranes and feed spacers for biofouling control. Water Res. 2012;46(12):3737-53.

Molin S & Tolker-Nielsen T. Gene transfer occurs with enhanced efficiency in biofilms and induces enhanced stabilisation of the biofilm structure. Curr Opin Biotechnol. 2003;14(3):266-61.

Norde W. Adsorption of proteins from solution at the solid-liquid interface. Adv Colloid Interface Sci. 1986;25:267-340.

Norde W. Driving forces for protein adsorption at solid surfaces. Macromol Symp. 1996;103(1):5–18.

Norde W. My voyage of discovery to proteins in flatland ...and beyond. Colloids Surf B Biointerfaces. 2008;61(1):1-9.

Oesterhelt F, Rief M & Gaub HE. Single molecule force spectroscopy by AFM indicates helical structure of poly(ethylene-glycol)in water. New J Phys 1. 1999:6.1-6.11.

Ohshima H, Fujita N & Kondo T. Adsorption kinetics with time delay. Colloid Polym Sci. 1992;270:707-10.

Ohshima H, Sato H, Matsubara H, Hyono A & Okubo M. A theory of adsorption kinetics with time delay and its application to overshoot and oscillation in the surface tension of gelatin solution. Colloid Polym Sci. 2004;282:1174-8.

Ostuni E, Chapman RG, Holmlin RE, Takayama S & Whitesides GM. A survey of structure-property relationships of surfaces that resist the adsorption of protein. Langmuir. 2001;17(18):5605-20.

Parbhu A, Hendy S & Danne M. Reducing milk protein adhesion rates: a transient surface treatment of stainless steel. Food Bioprod Process. 2006;84:274–8.

Pellenc D, Berry H & Gallet O. Adsorption-induced fibronectin aggregation and fibrillogenesis. J Colloid Interface Sci. 2006;298(1):132-44.

Petrone L. Molecular surface chemistry in marine bioadhesion. Adv Colloid Interface Sci. 2013;195-196:1-18.

Rabe M, Verdes D, Rankl M, Artus GR & Seeger S. A Comprehensive Study of Concepts and Phenomena of the Nonspecific Adsorption of β-Lactoglobulin. Chemphyschem. 2007;8(6):862–72.

Rabe M, Verdes D & Seeger S. Understanding protein adsorption phenomena at solid surfaces. Adv Colloid Interface Sci. 2011;162(1-2):87-106.

Ren, Y, Yang K & Zhang B. In vitro study of platelet adhesion on medical nickel-free stainless steel surface. Mater Lett. 2005;59(14-15):1785-9.

Satulovsky J, Carignano MA & Szleifer I. Kinetic and thermodynamic control of protein adsorption. Proc Nat Acad Sci USA. 1999;97(16):9037-41.

Spoering AL & Lewis K. Biofilms and planktonic cells of Pseudomonas aeruginosa have similar resistance to killing by antimicrobials. J Bacteriol. 2001;183:6746–51.

Sonato A, Silvestri D, Ruffato G, Zacco G, Romanato F & Morpurgo M. Quantitative control of poly(ethylene oxide) surface antifouling and biodetection through azimuthally enhanced grating coupled-surface plasmon resonance sensing. Appl Surf Sci. 2013;286:22-30.

Stoodley P, Sauer K, Davies DG & Costerton JW. Biofilms as complex differentiated communities. Annu Rev Microbiol. 2002;56:187–209.

Subbiahdoss G, Kuijer R, Grijpma DW, Van der Mei HC & Busscher HJ. Microbial biofilm growth vs. tissue integration: “the race for the surface” experimentally studied. Acta Biomater. 2009;5:1399–404.

Szleifer I. Protein adsorption on surfaces with grafted polymers: a theoretical approach. Biophys J. 1997;72(2 Pt 1):595-612.

Tabary N, Lepretre S, Boschin F, Blanchemain N, Neut C, Delcourt-Debruyne E, Martel B, Morcellet M & Hildebrand HF. Functionalization of PVDF membranes with carbohydrate derivates for the controlled delivery of chlorhexidin. Biomol Eng. 2007;24(5):472-6.

Talha M, Behera CK & Sinha OP. A review on nickel-free nitrogen containing austenitic stainless steels for biomedical applications. Mater Sci Eng C Mater Biol Appl. 2013;33(7):3563-75.

Tang X, Flint SH, Brooks JD & Bennett RJ. Factors affecting the attachment of micro-organisms isolated from ultrafiltration and reverse osmosis membranes in dairy processing plants. J Appl Microbiol. 2009;107(2):443–51.

Teitzel GM & Parsek MR. Heavy metal resistance of biofilm and planktonic Pseudomonas aeruginosa. Appl Environ Microbiol. 2003;69:2313–20.

Videla HA & Characklis WG. Biofouling and microbially influenced corrosion. Int. Biodeterior Biodegrad. 1992;29:195–212.

Vroman L & Adams AL. Findings with the recording ellipsometer suggesting rapid exchange of specific plasma proteins at liquid/solid interfaces. Surf Sci. 1969;16:438-46.

Vroman L, Adams AL & Klings M. Interactions among human blood proteins at interfaces. Fed Proc. 1971;30(5):1494-502.

Vroman L, Adams AL, Fischer GC & Munoz PC. Interaction of high molecular weight kininogen, factor XII, and fibrinogen in plasma at interfaces. Blood. 1980;55(1):156–9.

Walters MC, Roe F, Bugnicourt A, Franklin MJ & Stewart PS. Contributions of antibiotic penetration, oxygen limitation, and low metabolic activity to tolerance of Pseudomonas aeruginosa biofilms to ciprofloxacin and tobramycin. Antimicrob Agents Chemother. 2003;47:317–23.

Wang RLC, Kreuzer HJ & Grunze M. Molecular conformation and solvation of oligo(ethylene glycol)-terminated self-assembled monolayers and their resistance to protein adsorption. J Phys Chem B. 1997;101(47):9767–73.

Wei J, Ravn DB, Gram L & Kingshott P. Stainless steel modified with poly(ethylene glycol) can prevent protein adsorption but not bacterial adhesion. Colloids Surf B Biointerfaces. 2003;32(4):275-291.

Wertz CF & Santore MM. Adsorption and Reorientation Kinetics of Lysozyme on Hydrophobic Surfaces. Langmuir. 2002;18(4):1190–9.

Xu LC & Siedlecki CA. Effects of surface wettability and contact time on protein adhesion to biomaterial surfaces. Biomaterials. 2007;28(22):3273-83.

Yang Y, Rouxhet PG, Chudziak D, Telegdi J & Dupont-Gillain CC. Influence of poly(ethylene oxide)-based copolymer on protein adsorption and bacterial adhesion on stainless steel: Modulation by surface hydrophobicity. Bioelectrochemistry. 2014;97:127-36.

Yang YF, Hu HQ, Li Y, Wan LS, Xu ZK. Membrane surface with antibacterial property by grafting polycation. J Membr Sci. 2011;376(1-2):132-141.

Yoon RH, Flinn DH & Rabinovich YI. Hydrophobic interactionsbetween dissimilar surfaces. J Colloid Interface Sci. 1997;185(2):363–70.

Zhang M, Desai T & Ferrari M. Proteins and cells on PEG immobilized silicon surfaces. Biomaterials. 1998;19(10):953-60.